Journal of Applied Research on Industrial Engineering

www.journal-aprie.com

J. Appl. Res. Ind. Eng. Vol. 12, No. 1 (2024) 144–175.

Paper Type: Research Paper

Identification of Influential Parameters in Soil Liquefaction under Seismic Risk Using a Hybrid Neutrosophic Decision Framework

Avik Paul[1], Sima Ghosh[1], Priyanka Majumder[2,*], Surapati Pramanik[4], Florentin Smarandache[5]

[1] Department of Civil Engineering, National Institute of Technology Agartala, India; aviknit7@gmail.com; simacvl@gmail.com.
[2] Department of Basic Science and Humanities (Mathematics), Techno College of Engineering Agartala, Tripura, India; majumderpriyanka94@yahoo.com.
[3] Department of Mathematics, Nandalal Ghosh B. T. College, Panpur,Narayanpur, Dist- North 24 Parganas, West Bengal, India; surapati.math@gmail.com.
[4] University of New Mexico, Mathematics Department, 705 Gurley Ave., Gallup, NM 87301, USA; fsmarandache@gmail.com.

Citation:

Received: 23 October 2024 *Revised: 20 December 2024* *Accepted: 13 Januray 2025*	Paul, A., Ghosh, S., Majumder, P., Pramanik, S., & Smarandache, F. (2025). Identification of influential parameters in soil liquefaction under seismic risk using a hybrid neutrosophic decision framework. *Journal of applied research on industrial engineering, 12*(1), 144-175.

Abstract

Liquefaction of soil exposes buildings, bridges, and other vital infrastructure to structural failure, subsidence, and loss of bearing capacity during earthquakes. It can endanger safety and result in significant financial losses in seismically active areas. The objective of the present study is to identify the key factors influencing soil liquefaction is essential to improving the precision of risk assessment and mitigation plans in seismically active regions. An abrupt increase in pore water pressure leads to a significant fall in effective stress, which in turn causes a significant drop in shear strength. Soil liquefies, losing its ability to bear shear stresses and behaves as a fluid. To identify the key factors influencing soil liquefaction, an integrated Multi-Criteria Decision Making (MCDM) technique FUCOM-SVNN TOPSIS (Full Consistency Method (FUCOM), Single Valued Neutrosophic Number (SVNN), and Technique for Order of Preference by Similarity to Ideal Solution (TOPSIS)) has been developed. The study meticulously selects three key criteria and nine alternatives influenced by extensive literature review. Employing the FUCOM for establishing weights of criteria. FUCOM indicates that 'Seismic' is the most significant criteria. SVNN-TOPSIS applied for degerming the rank of alternatives. The results of SVNN-TOPSIS indicate that 'Peak Ground Acceleration' plays the crucial role in determining liquefaction potential. Validation of the proposed model by comparative study, statistical and sensitivity analysis, this methodology addresses the inherent uncertainties and interdependencies among various parameters, thereby enhancing the decision-making process related to seismic hazards.

Keywords: FUCOM, Liquefaction, MCDM, Single valued neutrosophic set, TOPSIS.

1 | Introduction

Liquefaction of soil is a crucial and intriguing subject in geotechnical-earthquake engineering, known for its complexity. It explains a process where dynamic forces such as blast loads, seismic vibrations, or sudden

Corresponding Author: majumderpriyanka94@yahoo.com
https://doi.org/10.22105/jarie.2024.486149.1699

external pressure cause loose, saturated, or partially saturated cohesionless soils to lose their stiffness and shear strength. This phenomenon results in an accumulation of pore water pressure due to undrained shearing, which lowers effective stress and drastically reduces shear strength. Because of this, the soil acts like a viscous liquid, which frequently causes heavier structures to sink and lighter ones to rise. The impacts of liquefaction can be catastrophic, including the formation of sand boils—where liquefied sand and water are expelled to the surface due to intense shaking—and structural failures. Additionally, land instability, such as sudden ground subsidence, is another severe consequence of this phenomenon. Several earthquakes have demonstrated the significant impact of soil liquefaction, including the Japan's 1964 Niigata earthquake (Mw 7.5) [1], The 1964 earthquake in Alaska (Mw 9.2) [2], the 1989 earthquake in the United States at Loma Prieta (Mw 6.9) [3], the 1995 Kobe earthquake in Japan (Mw 6.9) [4], the 1999 Chi-Chi earthquake in Taiwan (Mw 7.6) [5], and the 2001 Bhuj earthquake in India (Mw 7.7) [6].

In seismic zones, estimating the potential for liquefaction of soil layers beneath buildings and structures and determining treatment options for loose cohesionless soils necessitates sound engineering judgment [7]. In recent years, some researchers have developed cutting-edge semi-empirical processes [8] for evaluating soil liquefaction. The simplicity of field research makes it a common method of engineering evaluation. However, the variability in the input parameters related to soil and earthquake characteristics, and correlations only sometimes provide accurate findings. Recognizing uncertainties and their magnitude, as well as the sensitivity of analysis findings to changes in input parameters and technique utilized, can assist in selecting these variables and obtaining more trustworthy results.

Liquefaction is a critical concern in geotechnical earthquake engineering, recognized for its potential to cause significant damage. Numerous researchers have explored empirical methodologies to assess liquefaction potential triggered by various earthquake magnitudes. Andrus and Stokoe [7] applied a method involving shear wave velocity to examine liquefaction resistance, using data collected from 26 earthquakes, primarily in regions with alluvial soils containing silty clay layers. Youd et al. [8] proposed a streamlined approach that utilized parameters such as SPT, CPT, and shear wave velocity to predict liquefaction resistance. Cetin et al. [9] enhanced the field case history database and employed probabilistic techniques like Bayesian updating to identify correlations for liquefaction triggering. Sitharam et al. [10] combined laboratory and in-field assessments to study dynamic soil behavior under varying strain levels. Moss et al. [11] developed a methodology integrating probabilistic and deterministic approaches for liquefaction potential using CPT data, incorporating Bayesian regression for applications in performance-based engineering. Idriss and Boulanger [12] focused on semi-empirical methods for evaluating liquefaction in saturated cohesionless soils, drawing on extensive databases of SPT and CPT case histories. Later, Boulanger et al. [13] updated and refined the SPT-based liquefaction case history database, improving criteria using advanced seismic parameters like moment magnitudes and peak ground accelerations. Bhattacharya et al. [14] established semi-empirical correlations between SPT N-values and shear wave velocity specific to Kolkata's Rajarhat area, analyzing liquefaction potential through safety factor calculations. Mhaske and Choudhury [15] created a GIS-GPS soil property map of Mumbai, identifying high clay content areas prone to liquefaction. Chatterjee and Choudhury [16] developed empirical relationships between SPT N-values and shear wave velocity for Kolkata's varied soils, such as clay, silt, and silty sand, highlighting potential risks. Jakka et al. [17] computed safety factors for liquefaction at different depths in Kolkata, finding vulnerability in specific regions during a maximum credible earthquake of magnitude 5.4. Choudhury et al. [18] performed seismic liquefaction hazard analyses for pile designs in Mumbai, observing notable liquefaction potential in highly plastic clay soils. Desai and Choudhury [19] conducted ground response studies tailored for critical infrastructure, including ports and nuclear facilities in Mumbai. The Indian Standard Code IS 1893: Part 1 [20] offers a simplified guideline for evaluating liquefaction potential using SPT, CPT, and shear wave velocity. Sharma and Cheita [21] assessed liquefaction susceptibility in Guwahati by analyzing corrected SPT N-values through deterministic and probabilistic methods, noting soil compositions comparable to Kolkata's.Phule and Choudhury [22] mapped cyclic mobility in Mumbai's clayey soils using GIS tools, creating zonation maps for seismic liquefaction hazards. Chatterjee and Choudhury [23] performed ground response analyses in Kolkata to study local soil influences

on seismic behavior, emphasizing mitigation strategies against liquefaction. Nath et al. [24] examined historical and deterministic scenarios in Kolkata, referencing major earthquakes like the 1897 Shillong and 1934 Bihar-Nepal events, and concluded the city's soil properties favored liquefaction. Rao and Choudhury [25] assessed seismic risks for nuclear power plants, highlighting significant risks from high-magnitude earthquakes. Farichah [26] compared deterministic methods for liquefaction assessment in Taiwan, finding Cetin et al. [9] provided conservative estimates. Javdanian [27] introduced a novel approach using strain energy and gravitational search algorithms for liquefaction evaluation, demonstrating accurate predictions of vulnerable areas. Jha et al. [28] employed deterministic and probabilistic methods to assess liquefaction susceptibility, showing variability from low to high risk based on safety factors and liquefaction potential indices. Bandaru and Godavarthi [29] produced a preliminary liquefaction severity map for Andhra Pradesh. Singbal et al. [30] analyzed liquefaction using FOS at Mundra Port, India, employing CPT and DPT data. Rao and Choudhury [31] concentrated on probabilistic earthquake prediction and site analysis for a nuclear facility in Haryana. Sinha and Sarkar [32], [33] performed seismic hazard evaluations for Dhanbad, utilizing both deterministic and probabilistic approaches. Rao and Choudhury [34] analyzed seismic hazards in northwestern Haryana, utilizing deterministic techniques to quantify risks. These studies collectively underscore the importance of tailored, region-specific approaches to evaluating and mitigating liquefaction hazards. The First-Order Second-Moment (FOSM) approach was applied by Singnar and Sil [35] to assess Guwahati city's susceptibility to liquefaction. Das et al. [36] created LPI maps that took earthquake magnitudes into account for Agartala city. Ben-Zeev et al. [37] proposed a perspectives on the possibility of soil liquefaction under drained conditions, even at minimal seismic-energy density levels, shedding light on far-field liquefaction incidents that were not fully explained before. Hu and Wang [38] examined how data quality influences the effectiveness of machine learning models in assessing the liquefaction potential of gravelly soils. Additionally, uncertainties remain present in the data.

Other than this different researcher has been done different research on the key factors influencing soil liquefaction. Although numerous studies have explored the impact of various factors on liquefaction, limited attention has been given to systematically identifying the most significant ones. Seed and Idriss [39] highlighted five critical factors for predicting soil liquefaction: Soil Type (ST), relative density or void ratio, initial confining pressure, and the intensity and duration of ground shaking. Zhu [40] employed a Bayesian regression method to identify eight critical factors out of 15, which included normalized standard penetration blow count (SPTN), the groundwater table (D_w), critical layer depth (D_s), particle size (D50), impermeable capping layer thickness (H_n), nonuniformity coefficient (C_u), critical layer thickness (T_s), and frequency of the largest particle size. Dalvi et al. [41], using techniques like the Analytic Hierarchy Process (AHP) and entropy analysis, pinpointed eight essential factors—Mw, PGA, Peak Ground Velocity (PGV), frequency (f), normalized SPTN, vertical effective stress ($\sigma'V$), dynamic shear modulus, and relative density (Dr) from a total of 16. Tang et al. [42] expanded this work by identifying 12 significant factors out of 22 through bibliometric analysis, encompassing nearly all critical factors mentioned in prior research. Meanwhile, Lee and Hsiung [43] employed a multilayer perceptron neural network to evaluate factor sensitivities, finding that PGA was the most influential, with earthquake parameters like Mw and PGA being more sensitive to liquefaction than soil properties such as SPTN and Fines Content (FC). However, the conclusions across studies vary, with some methods, like the AHP and bibliometric analysis, being criticized for their subjectivity, which can introduce bias due to reliance on experience or sampling. On the other hand, more objective approaches, such as regression and neural network models, often neglect the interdependencies and mediation effects between factors, leading to less accurate assessments of their contributions to liquefaction. This limitation impacts the reliability of key factor identification and their true influence on liquefaction potential.

1.1 | Research Gap

A fundamental aspect of geotechnical earthquake engineering is comprehending how soil and foundation systems behave under dynamic loading circumstances, especially when dealing with crucial phenomena like liquefaction. Liquefaction, with its devastating impacts, necessitates accurate prediction and mitigation

strategies to safeguard infrastructure and human lives. While numerous methodologies—both deterministic and probabilistic—have been developed to evaluate the liquefaction potential of urban regions, these approaches often rely on simplified models. Deterministic methods typically focus on predefined parameters or threshold values, whereas probabilistic approaches aim to incorporate variability and uncertainties in soil properties and seismic inputs. Despite their widespread use, these methodologies frequently fall short of capturing the intricate interactions between a multitude of factors influencing soil behavior during seismic events. For instance, the effects of soil stratigraphy, grain size distribution, groundwater table fluctuations, epicentral distance and interaction between corrected SPT count with shear wave velocity are often oversimplified or overlooked entirely. Furthermore, the inherent complexity of urban soils, characterized by heterogeneity and a wide range of geotechnical properties, adds another layer of challenge to accurate liquefaction potential assessment. The interaction between these geotechnical parameters, environmental conditions, and site-specific seismic demands requires a more comprehensive and integrative evaluation framework. Thus, the existing research highlights a significant gap in developing robust, holistic methodologies that can seamlessly incorporate the interplay of influential factors into a unified model for assessing liquefaction potential. Addressing this gap is essential for improving predictive accuracy, refining mitigation strategies, and enhancing the resilience of urban infrastructure to seismic hazards.

1.2 | Objective

The objective of the research is to identify the influential parameters to assess the soil liquefaction. By identifying and ranking the critical factors influencing liquefaction potential, the study provides a robust framework for assessing seismic hazards and prioritizing mitigation strategies. A critical need in geotechnical earthquake engineering is to identify and rank the influential parameters for assessing soil liquefaction. There is a complex interplay between soil stratigraphy, grain size distribution, fluctuations in the groundwater table, corrected SPT count, and shear wave velocity when evaluating liquefaction, a phenomenon with devastating impacts on infrastructure and safety. Although widely used, existing methodologies often oversimplify these interactions or overlook critical parameters, leading to a lack of predictive accuracy. Geotechnical assessments of urban soils are further complicated by their inherent heterogeneity and diverse geotechnical properties. As a result of systematically identifying and prioritizing the factors that influence liquefaction potential, this study provides a more accurate assessment of seismic hazards. Through this approach, not only can the accuracy of seismic predictions be enhanced, but also targeted mitigation strategies can be developed, which ultimately enhances the resilience of urban infrastructure to seismic events.

The objective of the research is to identify the rank of alternatives by a new hybrid fuzzy based MCDM approach. With the introduction of fuzzy sets in 1965, Zadeh [44] made a substantial contribution to deal with uncertainty. Since then, numerous variations of fuzzy sets have emerged, all building on the core idea of fuzzy membership. For example, Torra's Hesitant Fuzzy Sets (HFSs) [45] allow for multiple membership degrees, while Intuitionistic Fuzzy Sets (IFSs) [46] incorporate both membership and non-membership degrees. Further extending IFSs [46], Atanassov and Gargov [47] developed interval-valued IFSs (IVIFSs) to better capture uncertainty with intervals rather than fixed values. Yager [48] developed the genertalised q-Rung Orthopair Fuzzy Set (q-ROFS) as an extension of fuzzy set that aimed to handle complex uncertainty and ambiguity in data. Pawlak [49] developed the rough set for dealing with uncertainty and incomplete information. Smarandache [50] developed the Neutrosophic Sets (NSs) to deal with uncertainty and indeterminacyby considering truth, indeterminacy, and falsity as independent components. However, due to the challenges in practical application and adoption of NSs, Wang et al. [51] proposed the Single Valued NSs (SVNSs), which offer greater practicality and flexibility. SVNSs [52] have proven effective in various domains, making them a valuable tool for handling complex data.

SVNNs [52] offer advantages in handling a broader range of uncertainties by explicitly representing indeterminacy, providing a simpler and more flexible approach to modeling uncertainty, and facilitating easier integration with other systems. Extensions of fuzzy sets such as IVIFSs [53], while flexible in handling intervals of membership and non-membership, do not address indeterminacy directly and may be more

complex to interpret and apply in situations involving high levels of indeterminacy. While q-ROFSs [48] provide detailed and granular information, their complexity and focus on membership and non-membership may make them less flexible in dealing with indeterminacy compared to SVNNs [51]. In contrast, rough set [49] excels in dealing with approximations and boundaries but do not address indeterminacy as explicitly or flexibly with respect to SVNNs [51].

The study relates neutrosophic principles to Zoroastrianism by relating neutrosophic notions of neutrality and indeterminacy with Zoroastrian dualism and moral beliefs. Most contemporary research focuses on binary opposites, such good and evil, often overlooking the nuances that lie in between. This study bridges the gap and offers a nuanced perspective on the interaction of opposites in Zoroastrianism by examining these conceptual uncertainties utilizing neutrosophic frameworks [54]. The implementation challenges of carbon credits, including funding, policy frameworks, and capacity building, have been examined in previous studies. A multi-criteria framework to rank these aspects according to their criticality is absent from these investigations, nevertheless. By using the IVSF-SWARA method to prioritize important elements and offer African countries practical insights, this study fills the gap and improves the application of carbon credits [55]. Although Linear Programming (LP) is frequently utilized in operations research for practical applications, decision-makers frequently encounter difficulties in achieving optimal solutions because of complexity and ambiguity. Neutosophic set theory has been presented as a method to deal with contradictory and ambiguous choice information in order to address these problems. Triangular Neutrosophic Numbers (TNNs) and other Neutrosophic Multi-Objective Linear Programming (NMOLP) issues are extremely difficult to solve. In order to close the gap in previous research, this paper suggests a novel method for solving NMOLP problems by converting them into equivalent crisp LP problems using a linear membership function [56]. The approximation of NSs and their relations to rough sets is one of the major additions to the existing research on rough set theory that has examined the usage of NSs to handle uncertainty. Fermatean Neutrosophic Sets (FNS) and Fermatean Neutrosophic Rough Sets (FNRS), as well as algebraic characteristics and approximation operators, have been proposed in recent works. By defining new Fermatean Neutrosophic Rough Approximation operators and examining their properties, this study seeks to fill the knowledge gap regarding the properties and applications of FNRS, specifically their cut sets and approximation operators [57]. In order to handle uncertainty, indeterminacy, and truth values in practical issues, previous research has concentrated on extending classical algebraic structures, such as G-modules, into the neutrosophic domain. Fuzzy and intuitionistic fuzzy G-modules, as well as neutrosophic G-modules and their characteristics, have been studied. Nevertheless, r-neutrosophic subsets of G-submodules, a particular class of NSs, and its algebraic properties are not well studied. By investigating the algebra of r-neutrosophic subsets of G-submodules, including their sum and structural features, this paper seeks to close that gap [58]. The use of Multi-Criteria Decision Analysis (MCDA) techniques, such as TOPSIS and OWA, to assess intricate decision-making situations, including judicial data protection, is highlighted in the literature. These approaches have been effectively used to deal with ambiguity and uncertainty in a variety of sectors, but they are limited in situations where subjective and unpredictable elements predominate. By presenting a neutrosophic-based TOPSIS-OWA framework to more accurately evaluate data protection tactics for procedural fairness in legal systems, this study closes this gap. The suggested approach improves decision-making in the face of ambiguity and captures the subtleties of indeterminacy, providing insightful information for enhancing judicial data protection [59]. Several limitations have been noted in previous studies on neutrosophic AHP group decision-making, especially with regard to the inability to preserve the reciprocal property of the neutrosophic trapezoidal pairwise comparison matrix. In order to overcome these limitations, this work suggests an enhanced neutrosophic AHP model that makes use of neutrosophic trapezoidal numbers. A thorough investigation demonstrates that the updated model outperforms the original approach in terms of accuracy and consistency. The study offers a more dependable method for complicated multi-criteria decision-making situations, which helps to improve decision-making in neutrosophic contexts [60]. Numerous extensions of fuzzy and neutrosophic graph theory have been investigated in order to represent indeterminacy and uncertainty in complex systems, including fuzzy mixed graphs and neutrosophic graphs. Nevertheless, in situations when indeterminacy is essential in both directed and undirected relationships, these

models frequently fall short. By adding truth, falsehood, and indeterminacy values to edge interactions, this study builds on earlier models to present the idea of Inverse Neutrosophic Mixed Graphs (INMG). The suggested INMG model offers a more sophisticated framework for network modeling in uncertain real-world scenarios, bringing fresh perspectives and potential uses, especially in social networks [61]. Data Envelopment Analysis (DEA) research has developed to deal with uncertainty, particularly through the use of fuzzy DEA and Neutrosophic DEA (Neu-DEA) models, which use fuzzy or neutrosophic numbers to assess Decision-Making Units (DMUs). Although these models enhance performance evaluation in unpredictable settings, there is still a need to use Pentagonal Neutrosophic Numbers (PNNs) to handle complicated degrees of uncertainty. By developing a new Pentagonal Neu-DEA model, adding PNNs to the inputs and outputs, and suggesting a new ranking function to transform the model into a clear LP model for more precise DMU performance measurement, this study closes this gap [62]. It has long been known that tourism may spur economic progress in developing nations by increasing competitiveness and implementing focused initiatives. Global crises, fierce competition, and substantial environmental changes, however, call for creative and flexible approaches to strategy selection. Traditional techniques, such as scenario-based planning and thorough analysis, find it difficult to handle the complexity and unpredictability of setting priorities for tourism strategy. By combining the Antifragility Analysis Algorithm (AAA) with NSs, this study fills the gap and makes it possible to evaluate strategies effectively in the face of uncertainty. By using this innovative method in the western part of Iran's Mazandaran Province, the study finds and ranks antifragile tourist tactics, providing a framework for optimizing gains in uncertain settings [63]. In mathematical programming, stochastic Multi-Objective Linear Programming (MOLP) problems—which frequently involve fluctuating coefficients and probabilistic constraints—are essential for simulating real-world uncertainty. Numerous approaches, including fuzzy sets, goal programming, and probabilistic approaches, are explored in existing research; nevertheless, these approaches have shortcomings when it comes to handling ambiguity and vagueness in data. Recent developments, such as the addition of NSs, integrate uncertainty through membership, non-membership, and indeterminacy functions, improving flexibility and realism. By creating a fuzzy goal programming framework in a neutrosophic setting, this study fills the gap and offers a more reliable and flexible approach to solving probabilistic MOLP problems under uncertainty [64]. In order to deal with uncertainty, current medical diagnosis techniques rely on fuzzy and intuitionistic fuzzy sets, however they are unable to manage inconsistent and ambiguous data. A strong framework for handling such complications is offered by neutrophilic sets, which are a generalization of fuzzy ideas and allow for increased diagnostic accuracy. Although previous research has introduced a number of measures, their actual medical applications frequently lack clarity and precision. By introducing a novel tan-log distance measure for single-valued NSs, this study fills the gap and provides a more accurate and efficient way to diagnose diseases while resolving the uncertainties present in existing techniques [65]. A major step forward in tackling performance assessment issues in settings with high data ambiguity and uncertainty is the combination of NSs and DEA. By adding three different membership degrees, Neu-DEA expands on traditional DEA and provides a more sophisticated framework for making decisions in unpredictable situations. Despite significant advancements in theoretical models and solution approaches for Neu-DEA, the application of these models to actual performance evaluation situations is still largely unexplored. By performing an extensive assessment of the Neu-DEA literature and identifying trends, limits, and future research opportunities to improve its applicability and efficacy in real-world scenarios, this study fills this crucial information vacuum [66]. Previous studies have highlighted the shortcomings of conventional statistical and fuzzy logic-based models in handling the intricacy and unpredictability of time series forecasting, especially their incapacity to account for data indeterminacy. Even while developments like meta-heuristic algorithms and generalized fuzzy sets have enhanced predictive power, reaching ideal accuracy still presents difficulties. By combining sophisticated optimization algorithms like QOA, GA, and PSO with neutrosophic logic—which includes true, false, and indeterminate components—this study fills the gap. The suggested NTS-QOA model advances the field with useful, accurate solutions by improving the representation of uncertainty and automating parameter selection, resulting in higher forecasting accuracy across a variety of datasets [67]. The limitations of conventional Multi-Attribute Decision-Making (MADM) techniques have been brought to light by the increasing complexity of

decision-making under uncertainty, especially when it comes to handling incomplete and ambiguous information. By combining Neutrosophic Triplets (NTs) with machine learning, this study fills these gaps and improves judgment accuracy, computational economy, and adaptability. By using this sophisticated framework for sustainable supplier selection, the study closes a significant gap in current approaches and offers a reliable way to assess options in challenging, unpredictable situations [68]. The majority of the current image completeness research focuses on techniques for restoring damaged areas by identifying the best data to substitute the absent portions while preserving visual coherence. These techniques, however, have problems with spatial and intensity ambiguities, which can result in problems such boundary discontinuities and inadequate homogeneity preservation. To overcome these obstacles, this paper suggests a novel method that uses neutrosophic-based segmentation. The approach improves patch matching for hole filling by lowering spatial and intensity ambiguities, providing better performance metrics than earlier methods. This study bridges the gap by using neutrosophic segmentation to provide more visually consistent and accurate image restoration [69].

The objective of the research is to identify the rank of alternatives by a new hybrid MCDM approach, namely, Full Consistency Method (FUCOM) [70] SVNN Technique for Order of Preference by Similarity to Ideal Solution (TOPSIS) [70] i.e. FUCOM-SVNN TOPSIS strategy. Identifying influential parameters for evaluating soil liquefaction is indeed crucial due to the uncertainties and the multitude of parameters involved. In this current investigation, the TOPSIS approach is employed to determine the optimal choice, guided by the principles outlined in the primary reference [71]. The TrF-FOCUM oversees the assignment of criteria weights, aiding in this decision-making process [72]. The decision to utilize TOPSIS in this study is based on its user-friendly nature and adaptability to address both qualitative and quantitative considerations. This methodology enhances the reliability of ranking outcomes by evaluating each option in terms of both its best and worst results. TOPSIS proves to be a versatile choice for material selection scenarios where the interaction between performance and cost is significant, as it accommodates cost-beneficial parameters. Despite extensive exploration of fuzzy and intuitionistic fuzzy Multiple Attribute Decision Making (MADM) problems by scholars, the integration of uncertainty into the model formulation remains a focal point. Recognizing the pivotal role of ambiguity in MADM challenges, the adoption of NSs becomes imperative to tackle complexities arising from uncertainty, indeterminacy, and inconsistency within the MADM methodology. While previous research has predominantly addressed fuzzy and intuitionistic fuzzy MADM challenges, the inclusion of indeterminacy within the MADM domain is considered essential. Biswas et al. [73–75] presented the TOPSIS strategy in the SVNN environment. Several neutrosophic-TOPSIS strategies have been developed to determine the ranking of alternatives, recognizing the need to address uncertainties, indeterminacies, and inconsistencies inherent in MADM difficulties in various neutrosophic environments like neutrosophic soft expert environment [76], rough neutrosophic environment [77], refined neutrosophic environment [78], bi-polar neutrosophic environment [79], neutrosophic cubic environment [80], trapezoidal neutrosophic numbers environment [81], neutrosophic number setting [82]. In 2023, Pramanik et al. [83], formulated the Best-Worst Method (BWM) TOPSIS strategy, specifically tailored for the SVNN environment. In 2024, Debroy et al. [83] presented triangular fuzzy BWM-neutrosophic-TOPSIS strategy under SVNS environment to select the most effective water quality parameter of aquaponic system. Rezaei [84] developed the BWM method to address certain limitations of the AHP [85]. Unlike AHP, BWM necessitates only 2n–3 pairwise comparisons, resulting in greater model consistency. Its flexibility extends beyond the constraint of comparing up to nine criteria, given the reduced number of required comparisons.

The inclusion of vectors like best-to-others as well as others-to-worst enhances the reliability of BWM results compared to AHP [85], which heavily relies on pairwise comparisons. However, BWM encounters challenges in determining appropriate weight coefficient values when faced with significant fluctuations affecting the consistency degree. It is advised in these situations to compute interval values as well as use the mean of these intervals as the final weight coefficient [85]. It is noteworthy that the central portion of the interval may or may not encompass values corresponding to the optimal weight coefficients, and interval weight values might not accurately represent optimal weights in cases of common inconsistency [86].

Various models have been proposed for determining criteria weights, with one notable example being the FUCOM [70] introduced by Pamučar et al. The FUCOM addresses deficiencies in both BWM and AHP models by facilitating pairwise comparisons of criteria with a manageable number of comparisons (precisely n – 1 comparisons). The FUCOM incorporates the decision-maker's subjective preferences into criteria weight determination, particularly in the initial steps involving criteria rating and pairwise comparisons. Despite its efficacy, the FUCOM exhibits modest variances in criteria weight values [35]. Importantly, it resolves the issue of repeated pairwise comparisons of criteria, as emphasized by Božanić et al. [87], Božanić et al. [88], and Durmić et al. [89].

The FUCOM approach is suggested for the purpose of calculating criteria weights since it emphasises maintaining consistency in expert judgements, ensuring legitimate and correct outputs in a straightforward and less computationally intensive way. However, because of its mathematical complexity, BWM is efficient but requires advanced tools; Ordinal Priority Approach (OPA) [57] can be computationally demanding because it depends on optimal pairwise comparisons; and Defining Interrelationships Between Ranked criteria (DIBR) [90] is highly complex and resource-intensive even though it accounts for interdependence among criteria. In contrast, Level Based Weight Assessment (LBWA)'s hierarchical structure [91] can be subjective and complex.

By computing the consistency index, which guarantees logical coherence in the pairwise comparisons of criteria weights, the FUCOM consistency in assessing the seismic parameter, site condition, and soil parameter the three liquefaction parameters are confirmed. By balancing accuracy and dependability, the approach checks to see if the ratios between the allocated weights meet predetermined consistency requirements. The chosen parameters in this study have consistency index values that stay within reasonable bounds, indicating that the weight allocations appropriately represent their relative importance. FUCOM's ability to generate accurate and consistent results that are specific to the assessment of soil liquefaction factors is guaranteed by this validation procedure.

By resolving the inherent uncertainties and complexities associated with nine essential parameters, such as Earthquake Magnitude, Ground Water Table, and Soil Plasticity, the SVNN-TOPSIS algorithm is modified to assess the liquefaction potential of soil. The uncertainty in the decision matrix is represented by Single-Valued Neutrosophic Numbers (SVNNs), which include degrees of truth, indeterminacy, and falsity for each parameter in question. The algorithm determines the separation measures from both the ideal and anti-ideal solutions using the weights obtained from FUCOM for the main criteria Seismic Parameter, Site Condition, and Soil Parameter ensuring a strong prioritization procedure. The methodology notably takes into account the geotechnical and seismic features of a location that is highly susceptible to liquefaction because of its alluvial soil and shallow groundwater table. This modification guarantees that the algorithm accurately determines the most important factors, addressing the uncertainties of liquefaction potential in a geologically complex and seismically active area.

This criteria-based approach, which integrates multiple influential factors for a comprehensive evaluation of soil liquefaction, can be adapted and applied to other geotechnical engineering problems, such as seismic hazard slope stability analysis, foundation design, and ground settlement prediction. Its applicability lies in its systematic framework that considers the interplay of site-specific parameters and external forces, ensuring a tailored and accurate assessment of geotechnical challenges.

1.3 | Novelty of the Study

The advantages of the developed strategy are presented below:

I. This study develops an innovative hybrid FUCOM-SVNN TOPSIS under SVNN environment. The weights of the criteria are determined using FUCOM, and the rank of the options is determined by SVNN-TOPSIS.

II. Due to the limited number of comparisons (n–1) at the criteria level, the proposed model minimizes errors in comparisons to the greatest extent possible.

III. Calculating the optimal values of criteria involves defining constraints.

IV. By explicitly accounting for degrees of truth, indeterminacy, and falsehood at the alternative level, the neutrosophic-TOPSIS strategy improves the robustness of the decision-making process to ambiguity. This guarantees the robustness of decision outcomes even when there are unclear or ambiguous information.

V. Although FUCOM-SVNN TOPSIS strategy under the SVNN environment methodologies have been used in a variety of fields, this work explicitly adapts the methodology to the evaluation of soil liquefaction potential. By taking into consideration the interaction of crucial elements including soil type, groundwater levels, and seismic activity, it makes use of the special qualities of a highly seismic location. A focus not before thoroughly examined within this methodological framework, the uncertainties and difficulties related to soil liquefaction are directly addressed by the approach thanks to this domain-specific adaption.

VI. In contrast to FUCOM-SVNN TOPSIS strategy under the SVNN environment generic uses, this study carries out a thorough literature analysis in order to choose nine options and three extremely pertinent criteria that are unique to soil liquefaction. This improvement offers a targeted and useful framework by bringing the decision-making process closer to the actual variables that affect liquefaction potential. In contrast to more generic implementations, the strategy exhibits enhanced precision in parameter prioritization by prioritizing seismic parameters over all others.

VII. Through scenario analysis and sensitivity analysis, the paper presents a twofold validation procedure that is not commonly highlighted in proposed hybrid method's applications. By guaranteeing that the approach is resistant to changes in input data and parameter uncertainty, these validations improve the robustness and dependability of the outputs. The suggested method is more resilient and flexible to real-world decision-making in dynamic and unpredictable situations, like those seen in seismic hazard assessments, thanks to this extra layer of dependability.

2 | Preliminaries of the SVNN

I. NSs were introduced by Smarandache [50], and Wang et al. [51] introduced SVNSs for dealing with ambiguous situations with partial information.

II. The following definition characterizes an SVNS ∂ over a predetermined set E:

$$U=\left\{\left(j,T_G(j),I_G(j),F_G(j)\right): j\in E\right\},$$

where $T_G: X\to\{0,1\}\cup(0,1)$, $I_G: X\to\{0,1\}\cup(0,1)$, $F_G: X\to\{0,1\}\cup(0,1)$ and so $0\le T_G(j)+I_G(j)+F_G(j)\le 3$. If an SVNS ∂ over given set E, we refer to the triplet $\left(T_G(j),I_G(j),F_G(j)\right)$ as an SVNN.

Mandal and Basu [92] introduced a novel score function to address MADM challenges within the SVNN framework, outlined as follows:

The scoring mechanism is established in the subsequent steps:

I. Assume that O represents the origin in a three-dimensional space, and $\Omega=\left(t_b,i_b,f_b\right)$, denotes as an SVNN, signifies a point within this space. Perform a translation of this point into Ω to arrive at $\Delta=\left(t_c,i_c,f_c\right)$. Here $t_c=t_b+\xi$, $i_c=i_b+\xi$, $f_c=f_b+\xi$, where $\xi>0$, each representing f_ε, a real number that remains distinct and unchanging throughout the specific problem, plays a crucial role. Now, we contemplate another point, $\Delta'=\left(t_c,-i_c,-f_c\right)$, which is the result of reflecting $\Delta=\left(t_c,i_c,f_c\right)$ across the *axis of x*, serving as a mirror.

II. Locate the score mapping $S_1(\Delta)=\cos\varpi$, with β representing the angle between $O\Delta$ and $O\Delta'$, and O denoting the origin.

III. If the score values for two distinct SVNNs, $\Delta_1=\left(t_{c_1},i_{c_1},f_{c_1}\right)$ and $\Delta_2=\left(t_{c_2},i_{c_2},f_{c_2}\right)$, denoted as $S_1(\Delta_1)$ and $S_1(\Delta_2)$ respectively, are equal, determine $\Delta_1^{**}=\left(t_{c_1},-i_{c_1},-\sqrt{f_{c_1}}\right)$ and $\Delta_2^{**}=\left(t_{c_2},-i_{c_2},-\sqrt{f_{c_2}}\right)$ respectively for the

corresponding translated points $\Delta_1^* = \left(t_{c_1^*}, i_{c_1^*}, f_{c_1^*}\right)$ and $\Delta_2^* = \left(t_{c_2^*}, i_{c_2^*}, f_{c_2^*}\right)$ where, $t_{c_1^*} = t_{c_1} + \xi, i_{c_1^*} = i_{c_1} + \xi,$ $f_{c_1^*} = f_{c_1} + \xi$ and $t_{c_2^*} = t_{c_2} + \xi, i_{c_2^*} = i_{c_2} + \xi, f_{c_2^*} = f_{c_2} + \xi$.

IV. Determine $\cos\phi$ and $\cos\psi$, where ϕ represents the angle between $O\Delta_1^*$ and $O\Delta_1^{**}$, and ψ signifies angle between $O\Delta_2^*$ as well as $O\Delta_2^{**}$, with O denoting the origin.

V. The score mapping $S_2(\Delta_1) = \cos\phi$ as well as $S_2(\Delta_2) = \cos\psi$.

3 | FUCOM-SVNN TOPSIS Strategy under the SVNN Environment

FUCOM-SVNN TOPSIS strategy under SVNN environment comprises two distinct phases. The initial phase involves a discussion on FUCOM to determine criteria weights. Subsequently, in the second phase, the focus shifts to discussing the neutrosophic TOPSIS strategy under SVNN environment, aimed at establishing the alternatives' rating. *Fig. 1* represents the computational steps of the proposed strategy. As shown in Fig 1, the blue-shaded sections represent FUCOM steps, the green-shaded section discusses SVNN-TOPSIS, and the yellow color represents the final output.

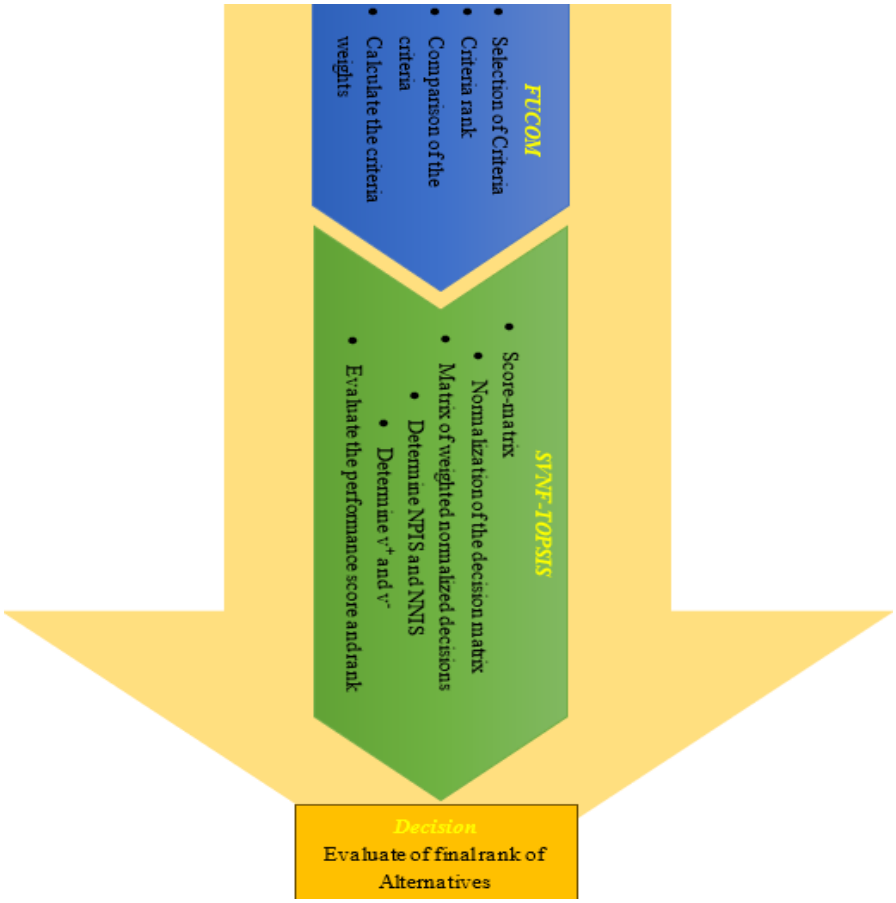

Fig 1. Flowchart of integrated MCDM strategy.

Phase 1. Full Consistency Method (FUCOM).

In the FUCOM, results are validated through pairwise comparisons and deviations from maximum consistency [70]. The key feature of FUCOM is that it can check the results by measuring the difference from optimum consistency in comparisons and by recognizing transferability in pairwise assessments of criteria. The decision-maker has an interpretive influence on the final weights assigned to the criteria under the

FUCOM model. Decision-makers rate the criteria in accordance with their preferences in *Steps 1* and *2* of FUCOM, and they next compare the ranked criteria pairwise. In contrast to subjective models, the FUCOM model has disclosed minor departures from a perfect value while establishing the weights of criterion [70]. Furthermore, FUCOM removes any redundancy found in subjective models by tackling overlaps in criteria comparisons while determining the weights of the criteria.

The FUCOM algorithm's stepwise method is described as follows:

Step 1. The first stage involves prioritizing the predetermined assessment criteria set $L=\{\Im_r : r=1(1)\mu\}$. Beginning with the criterion that is projected to have the highest weight coefficient and concluding with the criterion of least importance, this ranking is based on the estimated significance of each criterion. Consequently, the criteria have been arranged based on their anticipated weight coefficient values.

$$\Im_{r(1)} > \Im_{r(2)} > ... > \Im_{r(k)}.$$

The rank given to the evaluated criterion is indicated here by k. When two or more criteria are thought to be equally important, their equivalency is represented using the equality symbol (=) rather than the greater-than symbol (>).

Step 2. The second phase compares the rated criteria to ascertain their relative priority $\wp_{k/(k+1)}, k=1(1)\mu$, with k denoting the criteria's rank. The advantage of the criterion at rank $\wp_{k/(k+1)}$ over the criterion at rank $\Im_{r(k)}$ is represented by the relative priority $\Im_{r(k+1)}$. Consequently, as expression $\phi=\{\wp_{1/2},\wp_{2/3},...,\wp_{k/(k+1)}\}$ illustrates, the vectors of relative priorities for the evaluation criteria are established. The relevance (or priority) of the criterion-ranked $\wp_{k/(k+1)}$ relative to the criterion-ranked $\Im_{r(k+1)}$ is indicated here by the symbol $\Im_{r(k)}$.

One of the two approaches described in the following sections is used to establish the comparative priority of the criteria.

Sub-Step. 1. Decision-makers determine the comparative priority $\wp_{k/(k+1)}$ for the factors they are considering based on their personal preferences. In real-world applications, decision-makers use their internal knowledge to assess the rated criteria and assign the comparative priority $\wp_{k/(k+1)}$ according to personal preferences. The comparative priority is set to $\Im_{r(k+1)}$ if the decision-maker thinks that the criterion-ranked $\Im_{r(k)}$ is equally important to the criterion-ranked $\wp_{k/(k+1)}=1$.

Sub-Step. 2. Decision-makers assess the criteria to ascertain the importance of each criterion, as shown in expression $\Im_{r(1)} > \Im_{r(2)} > ... > \Im_{r(k)}$, using a predetermined scale for criterion comparison. The comparison is made in relation to the criterion that is ranked greatest in importance. As a result, all criteria ranked in *Step 1* have importance values $\partial_{\Im_{r(k)}}$. It follows that $\mu-1$ comparisons must be made since the highest-ranked criterion is compared to itself (with its significance set as $\partial_{\Im_{r(1)}}=1$).

Sub-Step-2 emphasizes how the FUCOM paradigm allows for pairwise comparisons of criteria using decimal, integer, or specified scale values created especially for these kinds of comparisons.

Step 3. The evaluation criterion $(\partial_1,\partial_2,...,\partial_\mu)^T$'s final weight coefficients are established in the third phase. The following two requirements must be fulfilled by these final weight values:

Restriction 1. As stated in *Step 2*, the weight coefficient ratio needs to match the comparative priority $\wp_{k/(k+1)}$ among the observed criteria. Stated otherwise, the following requirement needs to be met:

$$\partial_k/\partial_{k+1}=\wp_{k/(k+1)}.$$

Restriction 2. The final weight coefficients must meet the mathematical transitivity criteria in addition to condition $\partial_k/\partial_{k+1}=\wp_{k/(k+1)}$. In particular, the bond that $\wp_{k/(k+1)}\otimes\wp_{(k+1)/(k+2)}=\wp_{k/(k+2)}$ needs to maintain. $\left(\partial_k/\partial_{(k+1)}\right)\otimes\left(\partial_{(k+1)}/\partial_{(k+2)}\right)=\partial_k/\partial_{(k+2)}$ is the equation that is derived since $\wp_{k/(k+1)}=\partial_k/\partial_{(k+1)}$ and $\wp_{(k+1)/(k+2)}=\partial_{(k+1)}/\partial_{(k+2)}$. Consequently, the final weight coefficient values also need to meet the following requirement:

$$\partial_k/\partial_{(k+2)}=\left(\wp_k/\wp_{(k+1)}\right)\otimes\left(\wp_{(k+1)}/\wp_{(k+2)}\right).$$

Only when transitivity is completely maintained can full consistency, or minimum Deviation from Full Consistency (DFC) ς, be reached. When the requirements $\partial_k/\partial_{k+1}=\wp_{k/(k+1)}$ and $\partial_k/\partial_{(k+2)}=\wp_{k/(k+1)}\otimes\wp_{(k+1)/(k+2)}$ are met, something happens. This guarantees maximum consistency, therefore for the computed weight coefficients, $\varsigma=0$. The following inequalities must be met by the weight coefficients $\left(\partial_1,\partial_2,...,\partial_\mu\right)^T$ in order to meet these requirements: $\left|\partial_k/\partial_{k+1}-\wp_{k/(k+1)}\right|\le\varsigma$ and $\left|\partial_k/\partial_{(k+2)}-\wp_{k/(k+1)}\otimes\wp_{(k+1)/(k+2)}\right|\le\varsigma$. The need for greatest consistency is met by decreasing ς.

The final model for figuring out the weight coefficients of the evaluation criteria can be developed based on the parameters that have been defined.

$$\left.\begin{aligned}&\min\ \varsigma\\ &\text{subject to}\left|\frac{\partial_{r(k)}}{\partial_{r(k+1)}}-\wp_{k/(k+2)}\right|<\varsigma,\ \text{for all r}\\ &\left|\frac{\partial_{r(k)}}{\partial_{r(k+2)}}-\wp_{(k+1)/(k+2)}\right|<\varsigma,\ \text{for all r}\\ &\sum_r\partial_r=1\\ &\partial_r\ge 0,\ \text{for all r}\end{aligned}\right\}. \qquad (1)$$

The final values of the evaluation criterion $\left(\partial_1,\partial_2,...,\partial_\mu\right)^T$ and the degree of DFC $\varsigma=0$ are obtained by solving *Model (1)*. Two straightforward examples will demonstrate how to use FUCOM to determine weight coefficients in order to give a better understanding of the model. The first example illustrates how to use *Sub-Step-1* in *Step 2* to establish the comparative priority $\left(\wp_{k/(k+1)}\right)$, and the second example illustrates how to use *Sub-Step-2* in *Step 2* to determine $\wp_{k/(k+1)}$.

Phase 2. Neutrosophic TOPSIS strategy under SVNN environment.

Consider the set of alternatives $V=\{v_y:y=1(1)p\}$, $\tau\ge 1$ and $S=\{s_r:r=1(1)n\}$, $r\ge 2$ is the set of attributes with weights ∂_r, $r=1(1)n$ respectively.

Decision-makers assign ratings to the $q_y, y=1(1)p$ alternatives based on the attributes $s_r, r=1(1)n$, which are represented using SVNNs. The rating for the y^{th} attribute concerning the r^{th} alternative is presented as follows:

Assume that $v_y^*=\left(s_r,T_{v_y}(s_r),I_{v_y}(s_r),F_{v_y}(s_r)\right), y=1(1)p$, where $0\le T_{v_y}(s_r)+I_{v_y}(s_r)+F_{v_y}(s_r)\le 3$.

Here $\left(T_{yr}, I_{yr}, F_{yr}\right)$ is denoted as an SVNN. v_{yr}^{*}, $(y = 1(1)p$ and $r = 1(1)n)$, where r represents the number of attributes and τ represents the number of alternatives. Derive the decision matrix based on the ratings:

$\Gamma^{*} = \left[v_{yr}^{*}\right]_{p\times n}$

The TOPSIS approach can now be summed up as follows:

Step 1. Using $\Gamma^{*} = \left[v_{yr}^{*}\right]_{p\times n}$, $(y = 1(1)p$ and $r = 1, 2, ..., n$, and $r = 1, 2, ..., n)$ the scoring matrix $\Gamma = \left[v_{yr}\right]_{p\times n}$ is obtained from the decision matrix $v_{yr}^{*} = S_1\left(\left[v_{yr}\right]_{p\times n}\right)$.

Step 2. Determination of normalized decision matrix $\mho = \left[\lambda_{yr}\right]_{p\times n}$.

$$\text{Here} \quad \lambda_{yr} = \frac{v_{yr}^{*}}{\sqrt{\sum_{r=1}^{n} v_{yr}^{*}}}, , \; y = 1, 2, ..., p. \tag{2}$$

Step 3. The weighted normalized decision matrix $\Im = \left[\vartheta_{yr}\right]_{p\times n}$ is determined.

Here $\vartheta_{yr} = \partial_r \otimes \lambda_{yr}$, $y = 1, 2, ..., p$ and $r = 1, 2, ..., n$.

Step 4. Determine the NPIS (Neutrosophic Positive Ideal Solution) as well as NNIS (Neutrosophic Negative Ideal Solution) and is demoted by δ^{+} as well as δ^{-} respectively.

$\delta^{+} = \left\{\vartheta^{+}_{1}, \vartheta^{+}_{2}, ..., \vartheta^{+}_{n}\right\}$, where $\vartheta^{+}_{r} = \max_{r} \vartheta_{yr}, r = 1, 2, ..., n$.

$\delta^{-} = \left\{\vartheta^{-}_{1}, \vartheta^{-}_{2}, ..., \vartheta^{-}_{n}\right\}$, where $\vartheta^{-}_{r} = \min_{r} \vartheta_{yr}, r = 1, 2, ..., n$.

Step 5. Determine each alternative's distance from the NPIS and NNIS by applying the following *Formulas (3)* and *(4)*:

$$v_y^{+} = \sqrt{\sum_{r=1}^{n}\left(J_{yr} - \delta^{+}\right)^2}, y = 1, 2, ..., p, \tag{3}$$

$$v_y^{-} = \sqrt{\sum_{r=1}^{n}\left(J_{yr} - \delta^{-}\right)^2}, y = 1, 2, ..., p. \tag{4}$$

Step 6. Apply the *Formulas (3)* and *(4)* to determine every alternative's performance score:

$$R_y = v_y^{-} \Big/ \left(v_y^{+} + v_y^{-}\right) \qquad (5), y = 1, 2, ..., p. \tag{5}$$

4 | Methodology

This study's main objective is to decrease related uncertainty by determining the most important characteristics for evaluating soil liquefaction. The technique is divided into five sections: Section 4.1 discusses parameter selection; Section 4.2 applies the suggested MCDM; Section 4.3 is devoted to comparative study; Section 4.4 is devoted to statistical analysis; and Section 4.5 is devoted to sensitivity analysis. *Fig. 2* provides an overview of the complete technique.

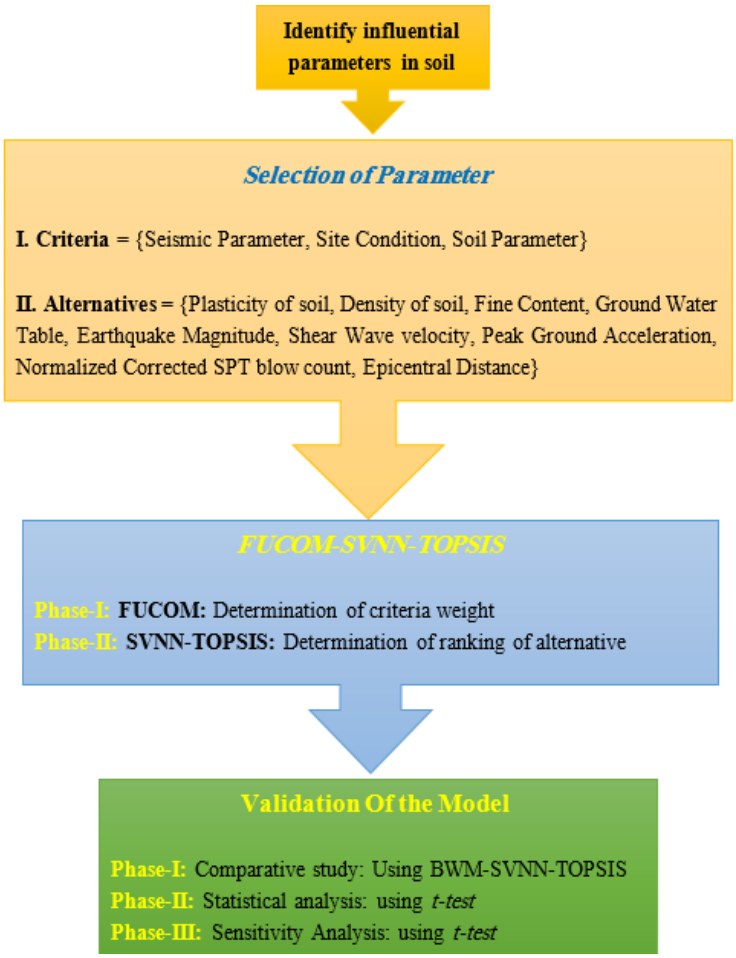

Fig. 2. Flowchart of the propose framework.

4.1 | Selection of Parameters

After expert as well as literature studies, nine factors affecting liquefaction potential were found. *Table 1* includes a range of criteria and options related to these factors. As the GWT table increases liquefaction potential increases. The higher plasticity indicates a higher fine content, which lowers the chances of liquefaction. As the epicentral distance increases energy dissipates more. So, the chances of liquefaction decrease. More the density higher is the effective stress so soil will provide more resistance to liquefaction. Peak ground acceleration is the acceleration at bed rock level which creates the inertia force for shaking. Higher the earthquake magnitude more is the energy release so higher is the chances of liquefaction. Higher the corrected SPT blow count, higher is the shear wave velocity and thus higher is the resistance against soil liquefaction.

Table 1. Selection of factors.

Criteria	Alternatives
Seismic Parameter $(\Im_1)$	Plasticity of soil (v_1)
Site Condition $(\Im_2)$	Density of soil (v_2)
Soil Parameter $(\Im_3)$	Fine content (v_3)
	Ground water table (v_4)
	Earthquake magnitude (v_5)
	Shear wave velocity (v_6)
	Peak ground acceleration (v_7)
	Normalized corrected SPT blow count (v_8)
	Epicentral distance (v_9)

4.2 | Application of Proposed MCDM

In this segment, two models are employed. *Model (1)* is utilized for ascertaining the criteria weights using the FUCOM method. *Model (2)* is applied to assess the score values of the alternatives through the neutrosophic TOPSIS strategy under SVNN environment.

4.2.1 | Application of Model (1)

In order of significance, the requirements are graded. The ranking is based on the consensus of the experts. In *Table 2*, comparisons are based on scales from 1 to 9.

$$s_1 > s_2 > s_3. \tag{6}$$

Table 2. Comparison of the importance of the evaluation criteria.

s_1	s_2	s_3
1	2.2	3

Calculate the relative importance of $\frac{\partial_1}{\partial_2} = 2.2$, $\frac{\partial_2}{\partial_3} = 1.36$, $\frac{\partial_1}{\partial_3} = 2.2 \times 1.36 = 2.99$ by comparing the obtained importance values.

The final weight of the coefficients can be found using the formula in *Eq. (7)*.

$$\left.\begin{aligned} &\min \varsigma \\ &\text{s.t.} \left|\frac{\partial_1}{\partial_2} - 2.2\right| \le \varsigma \\ &\left|\frac{\partial_2}{\partial_3} - 1.36\right| \le \varsigma \\ &\left|\frac{\partial_1}{\partial_3} - 2.99\right| \le \varsigma \\ &\partial_1 + \partial_2 + \partial_3 = 1 \\ &\partial_x \ge 0, \text{ for all } x = 1(1)3 \end{aligned}\right\}. \tag{7}$$

4.2.2 | Application of Model (2)

The decision maker utilizes SVNNs to assess alternatives based on their attributes, leading to the construction of the decision *Matrix 1*.

Matrix 1. Decision matrix.

$$\Gamma = \begin{array}{c} \\ v_1 \\ v_2 \\ v_3 \\ v_4 \\ v_5 \\ v_6 \\ v_7 \\ v_8 \\ v_9 \end{array} \begin{array}{c} \begin{array}{ccc} s_1 & s_2 & s_3 \end{array} \\ \begin{bmatrix} (0.89,0.43,0.11) & (0.93,0.34,0.12) & (0.88,0.21,0.19) \\ (0.81,0.49,0.21) & (0.85,0.29,0.20) & (0.79,0.44,0.10) \\ (0.79,0.24,0.24) & (0.97,0.36,0.12) & (0.77,0.17,0.19) \\ (0.75,0.46,0.26) & (0.93,0.24,0.17) & (0.78,0.24,0.27) \\ (0.83,0.28,0.02) & (0.88,0.36,0.23) & (0.80,0.20,0.13) \\ (0.79,0.32,0.06) & (0.78,0.20,0.16) & (0.94,0.46,0.12) \\ (0.80,0.30,0.07) & (0.87,0.30,0.15) & (0.91,0.29,0.08) \\ (0.95,0.24,0.26) & (0.90,0.32,0.17) & (0.95,0.47,0.23) \\ (0.73,0.33,0.20) & (0.72,0.14,0.15) & (0.70,0.15,0.24) \end{bmatrix} \end{array}.$$

Matrix Γ is translated by translating the entries of each entry. For each entry in matrix Γ, add 0.01 to all the components, represented in *Matrix 2*.

Matrix 2. Translation of Γ.

$$\begin{array}{c} \\ v_1 \\ v_2 \\ v_3 \\ v_4 \\ v_5 \\ v_6 \\ v_7 \\ v_8 \\ v_9 \end{array} \begin{array}{c} \begin{array}{ccc} s_1 & s_2 & s_3 \end{array} \\ \begin{bmatrix} (0.90,0.44,0.12) & (0.94,0.35,0.13) & (0.89,0.22,0.20) \\ (0.82,0.50,0.22) & (0.86,0.30,0.21) & (0.80,0.45,0.11) \\ (0.80,0.25,0.25) & (0.98,0.37,0.13) & (0.78,0.18,0.20) \\ (0.76,0.47,0.27) & (0.94,0.25,0.18) & (0.79,0.25,0.28) \\ (0.84,0.29,0.03) & (0.89,0.37,0.24) & (0.81,0.21,0.14) \\ (0.80,0.33,0.07) & (0.79,0.21,0.17) & (0.95,0.47,0.13) \\ (0.81,0.31,0.08) & (0.88,0.31,0.16) & (0.92,0.30,0.09) \\ (0.96,0.25,0.27) & (0.91,0.33,0.18) & (0.96,0.48,0.24) \\ (0.74,0.34,0.21) & (0.73,0.15,0.16) & (0.71,0.16,0.25) \end{bmatrix} \end{array}.$$

The next step is to determine the score matrix using the score function. *Matrix 3* represents the score matrix denoted by Γ^*. The score value of

$$S_1(0.90,0.44,0.12) = \frac{0.90\times 0.90 + 0.44\times(-0.44) + 0.12\times(-0.12)}{\sqrt{0.90^2+0.44^2+0.12^2}\sqrt{0.90^2+(-0.44)^2+(-0.12)^2}} = 0.591356,$$

Matrix 3. Score matrix.

$$\Gamma^{*} = \begin{array}{c} \\ v_1 \\ v_2 \\ v_3 \\ v_4 \\ v_5 \\ v_6 \\ v_7 \\ v_8 \\ v_9 \end{array} \begin{array}{c} \begin{array}{ccc} s_1 & s_2 & s_3 \end{array} \\ \begin{bmatrix} 0.591356 & 0.727468 & 0.799205 \\ 0.385249 & 0.69303 & 0.497777 \\ 0.673203 & 0.723927 & 0.787309 \\ 0.325683 & 0.80603 & 0.631634 \\ 0.784973 & 0.605717 & 0.823006 \\ 0.698063 & 0.790561 & 0.582917 \\ 0.729765 & 0.728379 & 0.792271 \\ 0.743803 & 0.708479 & 0.52381 \\ 0.548424 & 0.834423 & 0.702465 \end{bmatrix} \end{array}$$

Determine the normalized decision matrix using *Eq. (2)* on matrix Γ^{*}. As shown in *Matrix 4*, the normalized decision matrix is denoted by $\mho$.

$$\lambda_{11} = \frac{0.591356}{\sqrt{0.591356^2 + 0.385249^2 + 0.673203^2 + 0.325683^2 + 0.784973^2 + 0.698063^2 + 0.729765^2 + 0.743803^2 + 0.548424^2}} = 0.313972.$$

Matrix 4. Normalized decision matrix.

$$\mho = \begin{array}{c} \\ v_1 \\ v_2 \\ v_3 \\ v_4 \\ v_5 \\ v_6 \\ v_7 \\ v_8 \\ v_9 \end{array} \begin{array}{c} \begin{array}{ccc} s_1 & s_2 & s_3 \end{array} \\ \begin{bmatrix} 0.313972 & 0.328507 & 0.384607 \\ 0.204543 & 0.312955 & 0.239549 \\ 0.357428 & 0.326908 & 0.378883 \\ 0.172917 & 0.363983 & 0.303966 \\ 0.416771 & 0.273527 & 0.396061 \\ 0.370627 & 0.356998 & 0.280521 \\ 0.387459 & 0.328918 & 0.38127 \\ 0.394913 & 0.319932 & 0.252077 \\ 0.291178 & 0.376805 & 0.338053 \end{bmatrix} \end{array}.$$

4.3 | Comparative Study

Specialists are consulted to determine which vectors to use in BWM-neutrosophic TOPSIS strategy [82] under the SVNN environment and which aspects are most and least significant. In order to validate the proposed model, it was compared to a subjective model, namely the BWM-neutrosophic TOPSIS strategy under the SVNN environment approach. Comparisons were conducted based on pairwise evaluations of criteria, and results were validated using DFC. Based on the results, the proposed model outperforms the BWM-neutrosophic TOPSIS strategy under the SVNN environment method, especially when considering the relationship between consistency and the number of pairwise comparisons required. Over existing MCDM approaches, the proposed method has the following primary advantages: Compared to BWM-neutrosophic TOPSIS strategy under the SVNN environment, there are significantly fewer pairwise comparisons at the criteria level, comparing criteria pairwise in a consistent manner, enhancing rational decision-making by providing reliable criteria weight coefficients. As per expert consensus, S_1 is considered the best criterion, while S_2 is considered the worst. As the best-to-others vector is shown in *Table 3* and *Table 4* displays the vector that is worst-to-others.

Table 3. Best criteria compared to other criteria.

Best to Others	s_1	s_2	s_3
s_1	1	3	5

Table 4. To the worst criteria, there are other criteria.

Others to the Worst	s_3
s_1	5
s_2	4
s_3	1

Each criterion's weight can also be determined using the nonlinear mathematical *Model (8)*.

$$\left.\begin{aligned} &\min \varsigma \\ &\text{s.t.} \left|\frac{\partial_1}{\partial_2}-3\right|<\varsigma \\ &\left|\frac{\partial_1}{\partial_3}-5\right|<\varsigma \\ &\left|\frac{\partial_2}{\partial_3}-4\right|<\varsigma \\ &\sum_{x=1}^{3}\partial_x=1 \\ &\partial_x\geq 0, \text{ for all } x=1(1)3 \end{aligned}\right\}. \tag{8}$$

Eq. (2) can be used to find the normalized decision matrix for matrix Γ^*. The normalized decision matrix is represented as $\mho$, as can be seen in *Matrix 5*.

Matrix 5. Normalized decision matrix.

$$\mho = \begin{array}{c} \\ v_1 \\ v_2 \\ v_3 \\ v_4 \\ v_5 \\ v_6 \\ v_7 \\ v_8 \\ v_9 \end{array} \begin{array}{c} \begin{array}{ccc} s_1 & s_2 & s_3 \end{array} \\ \begin{bmatrix} 0.313972 & 0.328507 & 0.384607 \\ 0.204543 & 0.312955 & 0.239549 \\ 0.357428 & 0.326908 & 0.378883 \\ 0.172917 & 0.363983 & 0.303966 \\ 0.416771 & 0.273527 & 0.396061 \\ 0.370627 & 0.356998 & 0.280521 \\ 0.387459 & 0.328918 & 0.38127 \\ 0.394913 & 0.319932 & 0.252077 \\ 0.291178 & 0.376805 & 0.338053 \end{bmatrix} \end{array}.$$

4.4 | Statistical Analysis

When comparing rankings produced by the two approaches, the Spearman's rank correlation coefficient [93] is used to measure the linear relationship between the two variables. In the range of -1 to 1, a value of -1 indicates no linear correlation, a value of 0 indicates no correlation at all, and a value of 1 indicates perfect correlation. To evaluate the connection between variables on interval scales, Pearson's correlation coefficient [94] can be applied, as illustrated in *Eq. (9)*.

$$\rho(\kappa,\upsilon)=\frac{\mathrm{cov}(\kappa,\upsilon)}{\sigma_{\kappa}\sigma_{\upsilon}}. \quad (9)$$

κ As well as υ are covariant in $\mathrm{cov}(\kappa,\upsilon)$. SD is represented by κ as well as υ in both σ_{κ} as well as σ_{υ}.

The Pearson correlation coefficient is useful for evaluating the absence of a perfect correlation between two variables when it deviates from a value of 1.

$$\left.\begin{aligned} H_0 &: \rho \in (-\infty, 0] \\ H_1 &: \rho \in (0, \infty) \end{aligned}\right\}. \quad (10)$$

The Pearson correlation coefficient as well as the Student's t-distribution [95] with degrees of freedom (l – 1) are shown in *Eq. (10)*.

$$t=\rho\sqrt{\frac{\varepsilon-2}{1-\rho^{2}}}. \quad (11)$$

The hypothesis null hypothesis should be dismissed if t *Eq. (11)* exceeds $t_{\alpha}(l-2)$. The Pearson correlation coefficient ρ consists of the intervals l.

4.5 | Sensitivity Analysis

For soil liquefaction analysis, sensitivity analysis is essential because it determines how changes in input parameters affect the overall assessment of liquefaction potential. A number of interdependent factors play a role in soil liquefaction, including seismic parameters (e.g., earthquake magnitude and peak ground acceleration), site conditions (such as groundwater levels and soil density), and soil properties (such as plasticity and SPT blow count), all of which are subject to inherent uncertainty. As these parameters are systematically altered within realistic ranges, sensitivity analysis identifies the most influential factors driving the results, allowing a better understanding of their relative importance. Additionally, this process validates the robustness of the analysis as well as improves the accuracy of real-world liquefaction risk assessments by prioritizing data collection for the most important parameters.

To investigate the impact of altering weight coefficient values, various scenarios, each comprising a set, are examined. Sensitivity analysis is applied to evaluate the predominant criterion using *Eq. (12)* and ascertain the sensitivity of the criterion PVs (∂_x). The evolution of the dominant criterion is also explored. The updated weights found by the *Eqn. (12)* multiplied with each component of weighted normalized value in the *Step 3* in phase-II. After the calculation *Step 6* provides the updated score value of the alternatives for each random value used in the *Eq. (12)*.

$$\partial_x' = \partial_x\left(\frac{1-r\times\partial_B}{1-\partial_B}\right),\ x=1(1)3. \quad (12)$$

When ∂_x' represents the initial value of the criterion, denoted, $\partial_x(x=1(1)3)$; ∂_B, it signifies the criterion's starting point. $r_x \in (0,1)\cup\{0,1\}$,on the other hand, it represents the adjusted value.

5 | Result

Section 5 is divided into four subparts. In Section 5.1, the results of the proposed MCDM are presented. Section 5.2 presents the results of a comparative study. A statistical analysis is provided in Section 5.3. Sensitivity analysis results are presented in Section 5.4.

5.1 | Result from Proposed MCDM

This section discusses the weights of evaluating criteria as well as the ranking of evaluating alternatives.

5.1.1 | Result from FUCOM

The following are the ideal weights for the criterion, as derived by using the *Model (7)* solution.

$\partial_1^* = 0.5589605$, $\partial_2^* = 0.2541236$, $\partial_3^* = 0.1869159$, and $\varsigma^* = 0.4386387\mathrm{E}^{-03}$. Based on these weights, the Seismic Parameter (s_1) is identified as the most important criterion, while Soil Parameter (s_2) is deemed the least significant.

5.1.2 | Result in Neutrosophic TOPSIS strategy under SVNN environment

Once the weights of the criterion have been determined, compute the weighted normalized decision matrix. Multiply each criteria weight with the element of the corresponding row of matrix Ω to form the matrix. The weighted normalized decision matrix $\aleph$ is represented by the *Matrix 6*.

Matrix 6. Weighted Normalized decision matrix.

$$\Im = \begin{array}{c} \\ \mathrm{v}_1 \\ \mathrm{v}_2 \\ \mathrm{v}_3 \\ \mathrm{v}_4 \\ \mathrm{v}_5 \\ \mathrm{v}_6 \\ \mathrm{v}_7 \\ \mathrm{v}_8 \\ \mathrm{v}_9 \end{array} \begin{array}{c} \begin{array}{ccc} \mathrm{s}_1 & \mathrm{s}_2 & \mathrm{s}_3 \end{array} \\ \begin{bmatrix} 0.313972\times0.5589605 & 0.328507\times0.2541236 & 0.384607\times0.1869159 \\ 0.204543\times0.5589605 & 0.312955\times0.2541236 & 0.239549\times0.1869159 \\ 0.357428\times0.5589605 & 0.326908\times0.2541236 & 0.378883\times0.1869159 \\ 0.172917\times0.5589605 & 0.363983\times0.2541236 & 0.303966\times0.1869159 \\ 0.416771\times0.5589605 & 0.273527\times0.2541236 & 0.396061\times0.1869159 \\ 0.370627\times0.5589605 & 0.356998\times0.2541236 & 0.280521\times0.1869159 \\ 0.387459\times0.5589605 & 0.328918\times0.2541236 & 0.38127\times0.1869159 \\ 0.394913\times0.5589605 & 0.319932\times0.2541236 & 0.252077\times0.1869159 \\ 0.291178\times0.5589605 & 0.376805\times0.2541236 & 0.338053\times0.1869159 \end{bmatrix} \end{array}.$$

$$= \begin{array}{c} \\ \mathrm{v}_1 \\ \mathrm{v}_2 \\ \mathrm{v}_3 \\ \mathrm{v}_4 \\ \mathrm{v}_5 \\ \mathrm{v}_6 \\ \mathrm{v}_7 \\ \mathrm{v}_8 \\ \mathrm{v}_9 \end{array} \begin{array}{c} \begin{array}{ccc} \mathrm{s}_1 & \mathrm{s}_2 & \mathrm{s}_3 \end{array} \\ \begin{bmatrix} 0.175498 & 0.083481 & 0.071889 \\ 0.114331 & 0.079529 & 0.044775 \\ 0.199788 & 0.083075 & 0.070819 \\ 0.096654 & 0.092497 & 0.056816 \\ 0.232959 & 0.06951 & 0.07403 \\ 0.207166 & 0.090722 & 0.052434 \\ 0.216574 & 0.083586 & 0.071266 \\ 0.22074 & 0.081302 & 0.047117 \\ 0.162757 & 0.095755 & 0.063187 \end{bmatrix} \end{array}.$$

Next, determine NPIS and NNIS using $\vartheta^+_{\mathrm{r}} = \max_{\mathrm{r}} \vartheta_{\mathrm{yr}}, \mathrm{r} = 1(1)9$ and $\vartheta^-_{\mathrm{r}} = \min_{\mathrm{r}} \vartheta_{\mathrm{yr}}, \mathrm{r} = 1(1)9$ respectively.

$$\mathbf{J}^+_1 = \max\{0.175498, 0.114331, 0.199788, 0.096654, 0.232959, 0.207166, 0.216574, 0.22074, 0.162757\} = 0.232958,$$
$$\mathbf{J}^-_1 = \min\{0.175498, 0.114331, 0.199788, 0.096654, 0.232959, 0.207166, 0.216574, 0.22074, 0.162757\} = 0.0966537.$$

So,

$$\delta^+ = \{\mathbf{J}^+_1, \mathbf{J}^+_2, \mathbf{J}^+_3\} = \{0.232958, 0.0957550, 0.0740301\},$$
$$\delta^- = \{\mathbf{J}^-_1, \mathbf{J}^-_2, \mathbf{J}^-_3\} = \{0.0966537, 0.0695095, 0.0447754\}.$$

Afterwards, use *Formula (3)* as well as *Formula (4)* to calculate the distance between each alternative between NPIS as well as NNIS. The distances between each alternative between NPIS as well as NNIS are shown in *Table 5*.

Table 5. NPIS and NNIS distances from each alternative.

	NPIS Value		NNI Value
ν_1^+	0.058796	ν_1^-	0.084539
ν_2^+	0.123254	ν_2^-	0.02032
ν_3^+	0.035656	ν_3^-	0.107233
ν_4^+	0.137426	ν_4^-	0.02595
ν_5^+	0.026245	ν_5^-	0.139409
ν_6^+	0.034015	ν_6^-	0.11279
ν_7^+	0.020596	ν_7^-	0.123616
ν_8^+	0.032901	ν_8^-	0.124668
ν_9^+	0.071034	ν_9^-	0.073468

By applying *Formula (5)*, determine each alternative's performance score. The performance scores for each choice are shown in *Table 6*. Focussing on the alternatives' performance scores, arrange them in ascending order while assigning them ranks.

$$\begin{aligned} R_1 &= \nu_1^- \Big/ \left(\nu_1^+ + \nu_1^-\right), \\ &= 0.084539 \Big/ \left(0.058796 + 0.084539\right) \\ &= 0.589801. \end{aligned}$$

Table 6. Performance scores of alternatives.

Alternative	Performance Scores	Rank
R_1	0.589801	6
R_2	0.141529	9
R_3	0.750462	5
R_4	0.158834	8
R_5	0.841565	3
R_6	0.7683	4
R_7	0.857185	1
R_8	0.791196	2
R_9	0.508421	7

5.2 | Result of Comparative Study

In 2023, Pramanik et al. [83] introduced a strategy utilizing Neutrosophic BWM-TOPSIS under the SVNN environment. In real-world situations, the suggested FUCOM-SVNN-TOPSIS methodology has significant advantages over the BWM-SVNN-TOPSIS method, especially in situations like soil liquefaction studies where controlling uncertainty and maintaining methodological consistency are crucial. In order to ensure a better degree of consistency throughout the weight assignment process, FUCOM methodically assesses all pairwise comparisons, whereas BWM-SVNN-TOPSIS derives criteria weights by comparing only the best and worst criteria. This thorough consistency check guarantees more accurate weight derivation and minimizes any bias.

Furthermore, both approaches use SVNNs to manage uncertainty; but, the FUCOM-SVNN-TOPSIS technique incorporates FUCOM's improved consistency mechanism, which makes it more capable of handling the complex interrelationships between parameters, including soil, site, as well as seismic conditions.

The score values of the alternatives from the suggested technique are compared with those of the neutrosophic BWM-TOPSIS strategy within the SVNN environment, since the proposed method is based on the Neutrosophic-TOPSIS strategy under the SVNN environment.

Using the solution for *Model (8)*, optimal weights for the criteria are determined as follows: $\partial_1^* = 0.640000$, $\partial_2^* = 0.260000$, $\partial_3^* = 0.100000$, and $\varsigma^* = 0.14000$. Based on these weights, the seismic parameter (s_1) emerges as the most significant criterion, while the soil parameter (s2) is identified as the least significant.

Once the weights of the criteria have been established, compute the weighted normalized decision matrix. Multiply each criterion weight by the respective element in the corresponding matrix Ω row to generate the new matrix. This resulting matrix $\aleph$, denoted as *Matrix 7*, represents the weighted normalized decision matrix.

Matrix 7. Weighted normalized decision matrix.

$$\Im = \begin{array}{c} \\ v_1 \\ v_2 \\ v_3 \\ v_4 \\ v_5 \\ v_6 \\ v_7 \\ v_8 \\ v_9 \end{array} \begin{array}{c} \begin{array}{ccc} s_1 & s_2 & s_3 \end{array} \\ \begin{bmatrix} 0.313972\times 0.640000 & 0.328507\times 0.260000 & 0.384607\times 0.100000 \\ 0.204543\times 0.640000 & 0.312955\times 0.260000 & 0.239549\times 0.100000 \\ 0.357428\times 0.640000 & 0.326908\times 0.260000 & 0.378883\times 0.100000 \\ 0.172917\times 0.640000 & 0.363983\times 0.260000 & 0.303966\times 0.100000 \\ 0.416771\times 0.640000 & 0.273527\times 0.260000 & 0.396061\times 0.100000 \\ 0.370627\times 0.640000 & 0.356998\times 0.260000 & 0.280521\times 0.100000 \\ 0.387459\times 0.640000 & 0.328918\times 0.260000 & 0.38127\times 0.100000 \\ 0.394913\times 0.640000 & 0.319932\times 0.260000 & 0.252077\times 0.100000 \\ 0.291178\times 0.640000 & 0.376805\times 0.260000 & 0.338053\times 0.100000 \end{bmatrix} \end{array}.$$

$$= \begin{array}{c} \\ v_1 \\ v_2 \\ v_3 \\ v_4 \\ v_5 \\ v_6 \\ v_7 \\ v_8 \\ v_9 \end{array} \begin{array}{c} \begin{array}{ccc} s_1 & s_2 & s_3 \end{array} \\ \begin{bmatrix} 0.200942 & 0.085412 & 0.038461 \\ 0.130908 & 0.081368 & 0.023955 \\ 0.228754 & 0.084996 & 0.037888 \\ 0.110667 & 0.094636 & 0.030397 \\ 0.266734 & 0.071117 & 0.039606 \\ 0.237202 & 0.092819 & 0.028052 \\ 0.247974 & 0.085519 & 0.038127 \\ 0.252744 & 0.083182 & 0.025208 \\ 0.186354 & 0.097969 & 0.033805 \end{bmatrix} \end{array}.$$

Next determine NPIS and NNIS using $\vartheta^+_r = \max_r \vartheta_{yr}, r = 1(1)9$ and $\vartheta^-_r = \min_r \vartheta_{yr}, r = 1(1)9$ respectively.

$$\mathbf{J}^+_1 = \max\{0.200942, 0.130908, 0.228754, 0.110667, 0.266734, 0.237202, 0.247974, 0.252744, 0.186354\} = 0.266734,$$

$$\vartheta^-_1 = \min\{0.200942, 0.130908, 0.228754, 0.110667, 0.266734, 0.237202, 0.247974, 0.252744, 0.186354\} = 0.110667 \text{ So,}$$

$$\delta^+ = \{\mathbf{J}^+_1, \mathbf{J}^+_2, \mathbf{J}^+_3\} = \{0.266734, 0.097969, 0.039606\}.$$

$$| \ \delta^- = \{\mathbf{J}^-_1, \mathbf{J}^-_2, \mathbf{J}^-_3\} = \{0.110667, 0.071117, 0.023955\}.$$

From the NPIS and NNIS, use *Formulas (3)* and *(4)* to find the distance between each possibility. The resulting distances are shown in *Table 7*.

Table 7. NPIS and NNIS distances from each alternative.

	NPIS Value		NNIS Value
v_1^+	0.066989	v_1^-	0.092544
v_2^+	0.137729	v_2^-	0.022689
v_3^+	0.040171	v_3^-	0.119714
v_4^+	0.156374	v_4^-	0.024385
v_5^+	0.026852	v_5^-	0.15685
v_6^+	0.032127	v_6^-	0.128448
v_7^+	0.022564	v_7^-	0.138786
v_8^+	0.024934	v_8^-	0.142594
v_9^+	0.080589	v_9^-	0.080911

Calculate the evaluation score for each alternative using *Formula (5)*. *Fig. 3* illustrates the performance scores for each alternative by the proposed method and the existing methods.

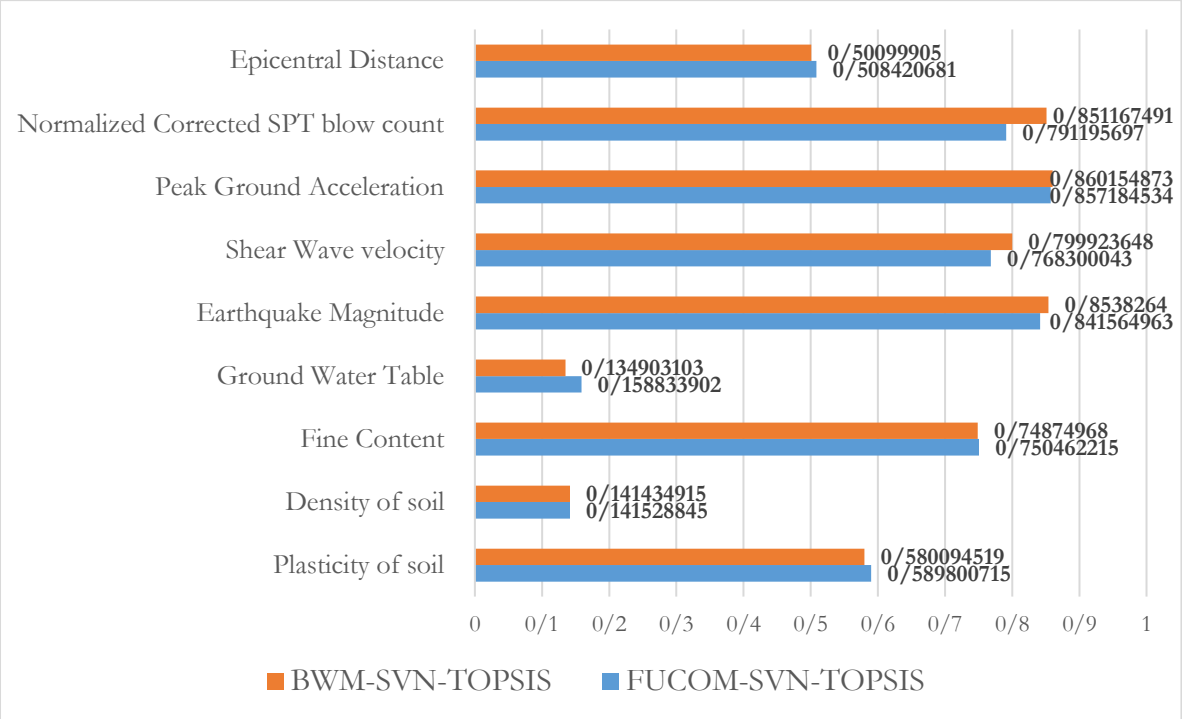

Fig. 3. Comparative study.

5.3 | Result of Statistical Analysis

The ranks produced by both techniques are assessed using the correlation coefficient [93]. A hypothesis test is not necessary if the rankings are the same and the Spearman's correlation value is 1. *Eq. (9)*, which describes a hypothesis test that may be carried out to validate the Spearman correlation coefficients [94], can be used if the rankings are different. To compare the proposed approach with the BWM-TOPSIS strategy under SVNN environment, the analysis employs the Pearson correlation coefficient [94] which is presented in *Table 8*.

Significantly, there is a noticeable correlation between the proposed PV models and the currently established PV models, supported by $\alpha = 0.05$. The findings from the analysis suggest that $t = \rho\sqrt{\frac{\varepsilon - 2}{1-\rho^2}}$ should outperform $t_{0.05}(1-2)$. A hypothesis test is conducted to confirm a positive correlation between the attributes of the existing and proposed methods.

Table 8. t-two-sample paired test for means.

	Variable 1	Variable 2
Mean	0.60081	0.607917075
Variance	0.078166	0.086689975
Observations	9	9
Pearson correlation	0.997523	
Hypothesized mean difference	0	
Df	8	
t Stat	-0.8506	
P(T<=t) one-tail	0.209859	
t Critical one-tail	1.859548	
P(T<=t) two-tail	0.419718	
t Critical two-tail	2.306004	

5.4 | Result of Sensitivity Analysis

Eq. (12) is utilized to create 25 unique scenarios for this study. Within these scenarios, the variable r is capable of adopting random values spanning from 0 to 1. *Fig. 4* shows the results of the sensitivity analysis. As shown in the *Fig. 4*, "Peak Ground Acceleration" is the most sensitive parameter in each case. Peak ground acceleration represents the maximum horizontal acceleration of the ground during an earthquake. It directly influences the inertia forces acting on soil particles, which drive the cyclic stresses that can trigger liquefaction. Higher PGA values correspond to stronger shaking and increased potential for pore pressure buildup in saturated soils. While it is not a property of the soil itself, PGA's role as a seismic loading factor makes it a critical external parameter influencing liquefaction susceptibility.

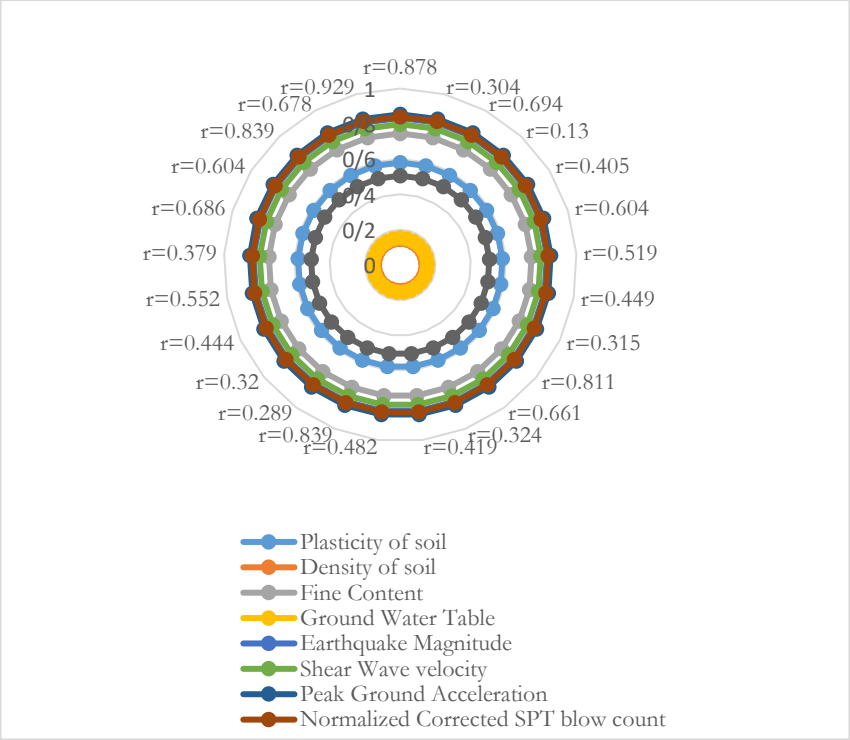

Fig. 4. Results of the sensitivity analysis.

6 | Discussion

The objective of the present study was to identify the influential parameters in soil liquefaction. To fulfil the objective, we have developed a hybrid MCDM technique namely FUCOM- SVNN TOPSIS strategy under the SVNN environment. Based on obtained results from FUCOM, we obtained that "Seismic Parameter" is the most significant criterion, with a weight of 0.607438. In the TOPSIS strategy under the SVNN environment, "Peak Ground Acceleration" scored 0.853869, making it the most significant alternative shown in *Table 6*. According to the BWM-TOPSIS strategy under the SVNN environment, "Peak Ground Acceleration" scored 0.860155, making it the most significant alternative, shown in *Fig. 1*. The next step is to determine whether the results of the suggested approach and the current method are correlated. Table 8 shows a very favorable result for the developed FUCOM-SVNN TOPSIS strategy since the t-value for the proposed method is lower than the t-value for the two-sample methods (2.306004). In this work, sensitivity analysis has been done to verify the model. "Peak Ground Acceleration" is the most sensitive parameter in each case (*Fig. 3*).

The present study advances the understanding of soil liquefaction by integrating the FUCOM-SVNN TOPSIS method for systematic ranking and prioritization of key factors, addressing the limitations of earlier studies. In the year 2021, Hu et al. identified 12 key factors, including Mw, PGA, Vs, and fines content, through an extensive review, while highlighting the contributions of Bayesian regression and entropy analysis in prior works for factor selection [96]. Uyanık in 2020 focused on earthquake parameters (Mw, dominant period, PGA) and soil parameters (fines content, density, shear wave velocity, groundwater depth) to predict liquefaction but lacked an integrated ranking approach [97]. In 2016, Tang et al. utilized bibliometric analysis and Interpretive Structural Modeling (ISM) to examine the interrelationships among 12 significant factors, emphasizing the direct impact of magnitude, epicentral distance, duration, and drainage conditions, with fines content as a pivotal parameter [42]. The present study, however, integrates seismic, site, and soil parameters and identifies Peak Ground Acceleration as the most critical factor using FUCOM to establish criteria weights and SVNN-TOPSIS for ranking. This provides a comprehensive, quantitative framework for liquefaction analysis, surpassing the qualitative and hierarchical methods of earlier works.

7 | Conclusion

This paper has developed a hybrid MCDM method namely FUCOM–SVNN TOPSIS Strategy under SVNN environment. The method was applied to identify the influential parameters in soil liquefaction. For this, the study has selected three criteria and nine alternatives through literature reviews. The results obtained from the developed FUCOM-SVNN TOPSIS strategy highlight thatthe 'Peak Ground Acceleration' is the most critical component.

The result was validated by comparing the proposed method with the BWM-SVNN TOPSIS strategy under the SVNN environment approach. The results of the proposed method, supported by the existing MCDM technique, are for the majority of significant alternatives. Statistical support is also provided for the results of the proposed method. Also, the model was validated by using sensitivity analysis and scenario analysis. According to the sensitivity analysis 'Peak Ground Acceleration' is the most sensitive parameter. In this study developed 25 different scenarios randomly. In each and every scenario the score value of 'Peak Ground Acceleration' is higher than all the considering parameters. So 'Peak Ground Acceleration' is more sensitive parameter. Peak ground acceleration represents the maximum horizontal acceleration of the ground during an earthquake. It directly influences the inertia forces acting on soil particles, which drive the cyclic stresses that can trigger liquefaction. Higher PGA values correspond to stronger shaking and increased potential for pore pressure buildup in saturated soils. While it is not a property of the soil itself, PGA's role as a seismic loading factor makes it a critical external parameter influencing liquefaction susceptibility.

The results presented offer significant contributions to the field of geotechnical engineering and seismic risk assessment, particularly in enhancing the understanding and prediction of soil liquefaction potential. By

identifying and ranking nine critical factors influencing liquefaction potential, the study provides a robust framework for assessing seismic hazards and prioritizing mitigation strategies. The ranking of factors highlights their relative importance, offering a valuable reference for engineers and researchers. For instance, parameters like shear wave velocity, normalized corrected SPT blow count, and peak ground acceleration (ranked 1st, 2nd, and 3rd respectively) demonstrate their dominant role in determining liquefaction resistance. The inclusion of diverse criteria—such as seismic parameters, soil properties, and site conditions—addresses the multifaceted nature of liquefaction, reducing oversimplifications often seen in traditional assessments. The performance scores linked to each factor help quantify their impact on liquefaction potential, leading to more precise risk assessments and enhanced predictive modelling.

Traditional methods for evaluating liquefaction potential often rely on simplified models that fail to consider the intricate interactions among various parameters. This approach enables a more accurate assessment by incorporating multiple influential factors, including normalized corrected SPT blow count, shear wave velocity, and fine content. A detailed evaluation helps in pinpointing high-risk areas, ensuring that the mitigation strategies are data-driven and site-specific.

This approach contributes to the development of probabilistic models for seismic risk assessment, which are more reliable due to the inclusion of influential parameters. The results can be integrated into decision-making tools to evaluate the safety of existing infrastructure against the soil liquefaction. Moreover, they contribute to creating detailed seismic hazard maps and refining probabilistic models for better disaster preparedness and decision-making.

Integrating influential parameters into a robust evaluation framework supports the creation of detailed seismic hazard maps. These maps not only delineate areas of high liquefaction susceptibility but also aid urban planners, policymakers, and emergency responders in developing risk management plans.

A comprehensive analysis of liquefaction factors directly contributes to disaster preparedness by enabling the development of effective mitigation measures. Techniques such as soil densification, installation of drainage systems, and grouting can be strategically applied to stabilize vulnerable sites. This preparedness minimizes the potential for catastrophic failures during seismic events.

The effect of criteria in this analysis is crucial because it allows for a weighted evaluation of the diverse and non-linear parameters influencing seismic soil liquefaction, including seismic parameters, site conditions, and soil properties. Assigning weights to these criteria helps capture their varying degrees of significance, ensuring a more accurate and nuanced evaluation of liquefaction potential. So, in feature a new approach can be developed to assess the soil liquefaction using MCDM so that the evaluated weight can be used to assess the soil liquefaction. This approach addresses the limitations of conventional methods, which may oversimplify or neglect critical factors, leading to a more reliable prediction of liquefaction risk and better-informed mitigation strategies. In feature developed an index to evaluate risk assessment of soil liquefaction. The index is developed the weightage of importance of considering factors of soil liquefaction risk. The weights will be determined by using MCDM techniques.

It is necessary to ensure strict consistency in pairwise comparisons according to the proposed model. Even small inconsistencies can require revising the entire judgment matrix, especially in problems with multiple criteria. By aggregating the inputs of a variety of experts, individual biases are minimized.

Conflict of Interest

The authors declare that they have no conflict of interest.

Data Availability

All data are included in the text.

Funding

This research received no specific grant from funding agencies in the public, commercial, or not-for-profit sectors.

References

[1] Kawasumi, H. (1968). *General report on the Niigata Earthquake of 1964*. Electrical Engineering College Press Tokyo, Japan. http://ds.iris.edu/seismo-archives/quakes/1964niigata/Kawasumi1968.pdf

[2] The Seismological Society of America. (1968). *The great alaska earthquake of 1964*. https://dggs.alaska.gov/webpubs/usgs/p/text/p0541.pdf

[3] Ma, K.-F., Satake, K., & Kanamori, H. (1991). The origin of the tsunami excited by the 1989 Loma Prieta Earthquake—Faulting or slumping? *Geophysical research letters*, *18*(4), 637–640. https://doi.org/10.1029/91GL00818

[4] Koketsu, K., Yoshida, S., & Higashihara, H. (1998). A fault model of the 1995 Kobe earthquake derived from the GPS data on the Akashi Kaikyo Bridge and other datasets. *Earth, planets and space*, *50*, 803–811. https://doi.org/10.1186/BF03352173

[5] Li, W. H., Lee, C. H., Ma, M. H., Huang, P. J., & Wu, S. Y. (2019). Fault dynamics of the 1999 Chi-Chi earthquake: clues from nanometric geochemical analysis of fault gouges. *Scientific reports*, *9*(1), 5683. https://doi.org/10.1038/s41598-019-42028-w

[6] Gupta, H. K., Harinarayana, T., Kousalya, M., Mishra, D. C., Mohan, I., Rao, N. P., … & Sarkar, D. (2001). Bhuj earthquake of 26 January, 2001. *Geological society of india*, *57*(3), 275–278. https://www.samvad.sibmpune.edu.in/index.php/jgsi/article/download/82432/63592

[7] Andrus, R. D., & Stokoe II, K. H. (2000). Liquefaction resistance of soils from shear-wave velocity. *Journal of geotechnical and geoenvironmental engineering*, *126*(11), 1015–1025. https://doi.org/10.1061/(ASCE)1090-0241(2000)126:11(1015)

[8] Youd, T. L., & Idriss, I. M. (2001). Liquefaction resistance of soils: summary report from the 1996 NCEER and 1998 NCEER/NSF workshops on evaluation of liquefaction resistance of soils. *Journal of geotechnical and geoenvironmental engineering*, *127*(4), 297–313. https://doi.org/10.1061/(ASCE)1090-0241(2001)127:4(297)

[9] Cetin, K. O., Seed, R. B., Der Kiureghian, A., Tokimatsu, K., Harder Jr, L. F., Kayen, R. E., & Moss, R. E. S. (2004). Standard penetration test-based probabilistic and deterministic assessment of seismic soil liquefaction potential. *Journal of geotechnical and geoenvironmental engineering*, *130*(12), 1314–1340. https://doi.org/10.1061/(ASCE)1090-0241(2004)130:12(1314)

[10] Sitharam, T. G., Govindaraju, L., & Sridharan, A. (2004). Dynamic properties and liquefaction potential of soils. *Current science*, *87*(10), 1370–1387. http://cs-test.ias.ac.in/cs/Downloads/article_38115.pdf

[11] Moss, R. E., Seed, R. B., Kayen, R. E., Stewart, J. P., Der Kiureghian, A., & Cetin, K. O. (2006). CPT-based probabilistic and deterministic assessment of in situ seismic soil liquefaction potential. *Journal of geotechnical and geoenvironmental engineering*, *132*(8), 1032–1051. https://doi.org/10.1061/(ASCE)1090-0241(2006)132:8(1032)

[12] Idriss, I. M., & Boulanger, R. W. (2008). *Soil liquefaction during earthquakes*. Earthquake Engineering Research Institute. https://istasazeh-co.com/wp-content/uploads/2023/02/Soil-Liquefaction-During-Earthquakes-M.-Idriss-and-Ross-W.-Boulanger.pdf

[13] Boulanger, R. W., Wilson, D. W., & Idriss, I. M. (2012). Examination and reevalaution of SPT-based liquefaction triggering case histories. *Journal of geotechnical and geoenvironmental engineering*, *138*(8), 898–909. https://doi.org/10.1061/(ASCE)GT.1943-5606.0000668

[14] Bhattacharya, P., Mukherjee, S. P., & Das, B. (2010). Prediction of liquefaction potential for Kolkata region by semi-empirical method. *International conferences on recent advances in geotechnical earthquake engineering and soil dynamics* (pp. 1-6). https://scholarsmine.mst.edu/icrageesd/05icrageesd/session04/32/

[15] Mhaske, S. Y., & Choudhury, D. (2011). GIS-GPS based map of soil index properties for Mumbai. *Geo-frontiers 2011: advances in geotechnical engineering* (pp. 2366–2375). American Society of Civil Engineers. https://doi.org/10.1061/41165(397)242

[16] Chatterjee, K., & Choudhury, D. (2013). Variations in shear wave velocity and soil site class in Kolkata city using regression and sensitivity analysis. *Natural hazards*, *69*, 2057–2082. https://doi.org/10.1007/s11069-013-0795-7

[17] Jakka, R. S., Shiuly, A., & Das, R. (2013). Liquefaction potential for Kolkata city. *International journal of geotechnical earthquake engineering (ijgee)*, *4*(2), 18–33. DOI: 10.4018/ijgee.2013070102

[18] Choudhury, D., Phanikanth, V. S., Mhaske, S. Y., Phule, R. R., & Chatterjee, K. (2015). Seismic liquefaction hazard and site response for design of piles in Mumbai city. *Indian geotechnical journal*, *45*, 62–78. https://doi.org/10.1007/s40098-014-0108-4

[19] Desai, S. S., & Choudhury, D. (2015). Site-specific seismic ground response study for nuclear power plants and ports in Mumbai. *Natural hazards review*, *16*(4), 4015002. https://doi.org/10.1061/(ASCE)NH.1527-6996.0000177

[20] IS, I. S. C. (1893). *2002 Criteria for earthquake resistant design of structure*. https://law.resource.org/pub/in/bis/S03/is.1893.1.2002.pdf

[21] Sharma, B., & Chetia, M. (2016). Deterministic and probabilistic liquefaction potential evaluation of Guwahati city. *Japanese geotechnical society special publication*, *2*(22), 823–828. https://doi.org/10.3208/jgssp.IND-32

[22] Phule, R. R., & Choudhury, D. (2017). Seismic reliability-based analysis and GIS mapping of cyclic mobility of clayey soils of Mumbai city, India. *Natural hazards*, *85*, 139–169. https://doi.org/10.1007/s11069-016-2570-z

[23] Chatterjee, K., & Choudhury, D. (2018). Influences of local soil conditions for ground response in Kolkata city during earthquakes. *Proceedings of the national academy of sciences, india section a: physical sciences*, *88*, 515–528. https://doi.org/10.1007/s40010-016-0265-1

[24] Nath, S. K., Srivastava, N., Ghatak, C., Adhikari, M. Das, Ghosh, A., & Sinha Ray, S. P. (2018). Earthquake induced liquefaction hazard, probability and risk assessment in the city of Kolkata, India: its historical perspective and deterministic scenario. *Journal of seismology*, *22*, 35–68. https://doi.org/10.1007/s10950-017-9691-z

[25] Rao, V. D., & Choudhury, D. (2018). Prediction of earthquake occurrence for a new nuclear power plant in India using probabilistic models. *Innovative infrastructure solutions*, *3*, 1–8. https://doi.org/10.1007/s41062-018-0185-9

[26] FFarichah, H. (2019, November). A comparative study of deterministic approach for assessing liquefaction potential. *IOP conference series: materials science and engineering* (Vol. 669, No. 1, p. 012041). IOP Publishing. DOI: 10.1088/1757-899X/669/1/012041

[27] Javdanian, H. (2019). Evaluation of soil liquefaction potential using energy approach: experimental and statistical investigation. *Bulletin of engineering geology and the environment*, *78*, 1697–1708. https://doi.org/10.1007/s10064-017-1201-6

[28] Jha, S. K., Karki, B., & Bhattarai, A. (2020). Deterministic and probabilistic evaluation of liquefaction potential: a case study from 2015 Gorkha (Nepal) earthquake. *Geotechnical and geological engineering*, *38*, 4369–4384. https://doi.org/10.1007/s10706-020-01277-7

[29] Bandaru, U. S., & Godavarthi, V. R. S. R. (2020). Seismic liquefaction potential assessment of andhra pradesh capital region. *Journal of earth system science*, *129*, 1–9. https://doi.org/10.1007/s12040-020-01403-2

[30] Singbal, P., Chatterjee, S., & Choudhury, D. (2020). Assessment of seismic liquefaction of soil site at Mundra Port, India, using CPT and DMT field tests. *Indian geotechnical journal*, *50*, 577–586. https://doi.org/10.1007/s40098-019-00395-1

[31] Rao, V. D., & Choudhury, D. (2020). Probabilistic modelling for earthquake forecasting in the northwestern part of Haryana state, India. *Pure and applied geophysics*, *177*(7), 3073–3087. https://doi.org/10.1007/s00024-020-02418-y

[32] Sinha, R., & Sarkar, R. (2020). Seismic hazard assessment of Dhanbad City, India, by deterministic approach. *Natural hazards*, *103*(2), 1857–1880. https://doi.org/10.1007/s11069-020-04059-9

[33] Sinha, R., & Sarkar, R. (2020). Probabilistic seismic hazard assessment of Dhanbad city, India. *Bulletin of engineering geology and the environment*, *79*(10), 5107–5124. https://doi.org/10.1007/s10064-020-01882-z

[34] Rao, V. D., & Choudhury, D. (2021). Deterministic seismic hazard analysis for the Northwestern Part of Haryana State, India, considering various seismicity levels. *Pure and applied geophysics*, *178*(2), 449–464. https://doi.org/10.1007/s00024-021-02669-3

[35] Singnar, L., & Sil, A. (2018). Liquefaction potential assessment of Guwahati city using first-order second-moment method. *Innovative infrastructure solutions*, *3*, 1–17. https://doi.org/10.1007/s41062-018-0138-3

[36] Das, S., Ghosh, S., & Kayal, J. R. (2019). Liquefaction potential of Agartala City in Northeast India using a GIS platform. *Bulletin of engineering geology and the environment*, *78*, 2919–2931. https://doi.org/10.1007/s10064-018-1287-5

[37] Ben-Zeev, S., Goren, L., Toussaint, R., & Aharonov, E. (2023). Drainage explains soil liquefaction beyond the earthquake near-field. *Nature communications*, *14*(1), 5791. https://doi.org/10.1038/s41467-023-41405-4

[38] Hu, J., & Wang, J. (2023). Influence of data quality on the performance of supervised classification models for predicting gravelly soil liquefaction. *Engineering geology*, *324*, 107254. https://doi.org/10.1016/j.enggeo.2023.107254

[39] Seed, H. B., & Idriss, I. M. (1971). Simplified procedure for evaluating soil liquefaction potential. *Journal of the soil mechanics and foundations division*, *97*(9), 1249–1273. https://doi.org/10.1061/JSFEAQ.0001662

[40] Zhu, S. (1981). Mathematic-statistical prediction of liquefaction of soil during an earthquake. *Seismology and geology*, *3*(2), 71–82.

[41] Dalvi, A. N., Pathak, S. R., & Rajhans, N. R. (2014). Entropy analysis for identifying significant parameters for seismic soil liquefaction. *Geomechanics and geoengineering*, *9*(1), 1–8. https://doi.org/10.1080/17486025.2013.805255

[42] Tang, X. W., Hu, J. L., & Qiu, J. N. (2016). Identifying significant influence factors of seismic soil liquefaction and analyzing their structural relationship. *KSCE journal of civil engineering*, *20*, 2655–2663. https://doi.org/10.1007/s12205-016-0339-2

[43] Lee, C. J., & Hsiung, T. K. (2009). Sensitivity analysis on a multilayer perceptron model for recognizing liquefaction cases. *Computers and geotechnics*, *36*(7), 1157–1163. https://doi.org/10.1016/j.compgeo.2009.05.002

[44] Zadeh, L. A. (1965). Information and control. *Fuzzy sets*, *8*(3), 338–353. https://www.sciencedirect.com/science/article/pii/S001999586590241X

[45] Torra, V. (2010). Hesitant fuzzy sets. *International journal of intelligent systems*, *25*(6), 529–539. https://doi.org/10.1002/int.20418

[46] Atanassov, K. T., & Atanassov, K. T. (1999). *Interval valued intuitionistic fuzzy sets*. Springer. https://link.springer.com/chapter/10.1007/978-3-7908-1870-3_2

[47] Atanassov, K., & Gargov, G. (1989). Interval valued intuitionistic fuzzy sets. *Fuzzy sets syst*, *31*(3), 343–349. DOI:10.1007/s12652-020-02227-0

[48] Yager, R. R. (2016). Generalized orthopair fuzzy sets. *IEEE transactions on fuzzy systems*, *25*(5), 1222–1230. https://doi.org/10.1109/TFUZZ.2016.2604005

[49] Pawlak, Z. (1982). Rough sets. *International journal of computer & information sciences*, *11*, 341–356. https://doi.org/10.1016/j.ins.2006.06.006

[50] Samrandache, F. (1999). *A unifying field in logics, Neutrosophy: Neutrosophic probability, set and logic, rehoboth*. Infinite Study.

[51] Wang, H., Smarandache, F., Zhang, Y., & Sunderraman, R. (2010). *Single valued neutrosophic sets*. Infinite study. https://books.google.nl/books

[52] Pramanik, S. (2022). Single-valued neutrosophic set: an overview. *Transdisciplinarity*, 563–608. https://doi.org/10.1007/978-3-030-94651-7_26

[53] Burillo, P., & Bustince, H. (1996). Entropy on intuitionistic fuzzy sets and on interval-valued fuzzy sets. *Fuzzy sets and systems*, *78*(3), 305–316. https://doi.org/10.1016/0165-0114(96)84611-2

[54] Smarandache, F. (2024). *The dynamic interplay of opposites in zoroastrianism*. Infinite Study. https://books.google.com/books

[55] Su, Q., Qiu, Y. J., Bouraima, M. B., Zonon, B. I. P., Badi, I., & Maraka, N. K. (2024). Addressing the crucial factors affecting the implementation of carbon credit concept using a comprehensive decision-making analysis: A case study. *Journal operation strateght analysis*, *2*(3), 136–143. https://www.researchgate.net

[56] Wang, Q., Huang, Y., Kong, S., Ma, X., Liu, Y., Das, S. K., & Edalatpanah, S. A. (2021). A novel method for solving multiobjective linear programming problems with triangular neutrosophic numbers. *Journal of mathematics*, *2021*(1), 6631762. https://doi.org/10.1155/2021/6631762

[57] Bhuvaneshwari, S., Crispin Sweety, C. A., & Sumathi, R. (2024). Fermatean neutrosophic rough set. *Computational algorithms and numerical dimensions*, *3*(4), 308–323. https://doi.org/10.22105/cand.2024.482087.1153

[58] Binu, R. (2024). R-neutrosophic subset of G-submodules. *Big data and computing visions*, *4*(2), 164–169. https://www.bidacv.com/article_206030_434e9e42b49d35eff0a794022c497194.pdf

[59] Ayala Ayala, L. R., Hernández Ramos, E. L., & Contento Correa, S. A. (2024). Neutrosophic TOPSIS-OWA framework for evaluating data protection strategies in judicial systems. *Journal of fuzzy extension and applications*, *5*(Spec. Issue), 1–11. https://doi.org/10.22105/jfea.2024.468198.1545

[60] Bhat, S. A. (2023). An enhanced AHP group decision-making model employing neutrosophic trapezoidal numbers. *Journal operation strateght analysis*, *1*(2), 81–89. https://library.acadlore.com/JOSA/2023/1/2/JOSA_01.02_05.pdf

[61] Jayaprakash, T., & Charles Selvaraj, A. C. S. (2024). Inverse neutrosophic mixed graphs. *Journal of fuzzy extension and applications*, *5*(3), 395–415. https://doi.org/10.22105/jfea.2024.429140.1356

[62] Mohanta, K. K., & Toragay, O. (2023). Enhanced performance evaluation through neutrosophic data envelopment analysis leveraging pentagonal neutrosophic numbers. *Journal of operational and strategic analytics*, *1*(2), 70–80. https://www.researchgate.net

[63] Ghaforiyan, M., Sorourkhah, A., & Edalatpanah, S. A. (2024). Identifying and prioritizing antifragile tourism strategies in a neutrosophic environment. *Journal of fuzzy extension and applications*, *5*(3), 374–394. https://doi.org/10.22105/jfea.2024.456894.1470

[64] Edalatpanah, S. A., Khalifa, H. A. E. W., Al-Quran, A., Al-Sharqi, F., Rodzi, Z., Lutfi, A., & others. (2023). Enhancing neutrosophic fuzzy goal programming approach for solving multi-objective probabilistic linear programming problems. *Full length article*, *23*(1), 311-322. https://www.researchgate.net/

[65] Samuel, A. E., & others. (2024). Enhancing medical diagnosis with single valued neutrosophic sets and Tan-log distance. *Soft computing fusion with applications*, *1*(1), 49–57. https://doi.org/10.22105/bep1t867

[66] Mohanta, K. K., & Sharanappa, D. S. (2023). Neutrosophic data envelopment analysis: a comprehensive review and current trends. https://doi.org/10.22105/opt.v1i1.19

[67] Edalatpanah, S. A., Hassani, F. S., Smarandache, F., Sorourkhah, A., Pamucar, D., & Cui, B. (2024). A hybrid time series forecasting method based on neutrosophic logic with applications in financial issues. *Engineering applications of artificial intelligence*, *129*, 107531. https://doi.org/10.1016/j.engappai.2023.107531

[68] Nafei, A., Azizi, S. P., Edalatpanah, S. A., & Huang, C. Y. (2024). Smart TOPSIS: a neural Network-Driven TOPSIS with neutrosophic triplets for green Supplier selection in sustainable manufacturing. *Expert systems with applications*, *255*, 124744. https://doi.org/10.1016/j.eswa.2024.124744

[69] Talouki, A. G., Koochari, A., & Edalatpanah, S. A. (2024). Image completion based on segmentation using neutrosophic sets. *Expert systems with applications*, *238*, 121769. https://doi.org/10.1016/j.eswa.2023.121769

[70] Pamučar, D., Stević, Ž., & Sremac, S. (2018). A new model for determining weight coefficients of criteria in mcdm models: Full consistency method (FUCOM). *Symmetry*, *10*(9), 2-22. https://doi.org/10.3390/sym10090393

[71] Hwang, C. L., Yoon, K., Hwang, C. L., & Yoon, K. (1981). Methods for multiple attribute decision making. In *Multiple attribute decision making: methods and applications a state-of-the-art survey* (pp. 58–191). Springer. https://doi.org/10.1007/978-3-642-48318-9_3

[72] Majumder, P. (2023). An integrated trapezoidal fuzzy FUCOM with single-valued neutrosophic fuzzy MARCOS and GMDH method to determine the alternatives weight and its applications in efficiency analysis of water treatment plant. *Expert systems with applications*, *225*, 120087. https://doi.org/10.1016/j.eswa.2023.120087

[73] Biswas, P., Pramanik, S., & Giri, B. C. (2016). TOPSIS method for multi-attribute group decision-making under single-valued neutrosophic environment. *Neural computing and applications*, *27*(3), 727–737. https://doi.org/10.1007/s00521-015-1891-2

[74] Biswas, P., Pramanik, S., & Giri, B. C. (2019). NonLinear programming approach for single-valued neutrosophic TOPSIS method. *New mathematics and natural computation*, *15*(02), 307–326. https://doi.org/10.1142/S1793005719500169

[75] Biswas, P., Pramanik, S., & Giri, B. C. (2019). Neutrosophic TOPSIS with group decision making. *Fuzzy multi-criteria decision-making using neutrosophic sets*, 543–585. https://doi.org/10.1007/978-3-030-00045-5_21

[76] Pramanik, S., Dey, P. P., & Giri, B. C. (2015). TOPSIS for single valued neutrosophic soft expert set based multi-attribute decision making problems. *Neutrosophic sets and systems*, *10*, 88–95. https://books.google.nl/books

[77] Mondal, K., Pramanik, S., & Smarandache, F. (2016). Rough neutrosophic TOPSIS for multi-attribute group decision making. *Infinite study*, *13*, 105-117. https://books.google.nl/books

[78] Pramanik, S., Banerjee, D., & Giri, B. C. (2016). *TOPSIS approach for multi attribute group decision making in refined neutrosophic environment*. Infinite Study. https://fs.unm.edu/TOPSISApproachForMultiAttribute.pdf

[79] Dey, P. P., Pramanik, S., & Giri, B. C. (2016). TOPSIS for solving multi-attribute decision making problems under bi-polar neutrosophic environment. In *New trends in neutrosophic theory and applications* (pp. 65–77). PONS Edition. https://books.google.nl/books

[80] Pramanik, S., Dey, P. P., Giri, B. C., & Smarandache, F. (2017). *An extended TOPSIS for multi-attribute decision making problems with neutrosophic cubic information*. Infinity Study. https://books.google.nl/books

[81] Biswas, P., Pramanik, S., & Giri, B. C. (2018). TOPSIS strategy for multi-attribute decision making with trapezoidal neutrosophic numbers. *Neutrosophic sets and systems*, *19*(1), 29–39. https://books.google.nl/books

[82] Mondal, K., Pramanik, S., & Giri, B. C. (2021). NN-TOPSIS strategy for MADM in neutrosophic number setting. *Neutrosophic sets and systems*, *47*, 66–92. https://books.google.nl/books

[83] Debroy, P., Majumder, P., Pramanik, S., & Seban, L. (2024). TrF-BWM-Neutrosophic-TOPSIS strategy under svns environment approach and its application to select the most effective water quality parameter of aquaponic system. *Neutrosophic sets and systems*, *70*(1), 13. https://digitalrepository.unm.edu/nss_journal/vol70/iss1/13/

[84] Rezaei, J. (2015). Best-worst multi-criteria decision-making method. *Omega*, *53*, 49–57. https://doi.org/10.1016/j.omega.2014.11.009

[85] Saaty, T. L. (n.d.). *Decision making for leaders: the analytic hierarchy process for decisions in a complex world*. RWS Publications. https://books.google.com/books

[86] Pamučar, D., Lukovac, V., Božanić, D., & Komazec, N. (2018). Multi-criteria FUCOM-MAIRCA model for the evaluation of level crossings: case study in the Republic of Serbia. *Operational research in engineering sciences: theory and applications*, *1*(1), 108–129. https://doi.org/10.31181/oresta190120101108p

[87] Bozanic, D., Tešić, D., & Kočić, J. (2019). Multi-criteria FUCOM–Fuzzy MABAC model for the selection of location for construction of single-span bailey bridge. *Decision making: applications in management and engineering*, *2*(1), 132-146. https://doi.org/10.31181/dmame1901132b

[88] Božanić, D., Tešić, D., & Milić, A. (2020). Multicriteria decision making model with Z-numbers based on FUCOM and MABAC model. *Decision making: applications in management and engineering*, *3*(2), 19–36. https://www.researchgate.net

[89] Durmić, E., Stević, Ž., Chatterjee, P., Vasiljević, M., & Tomašević, M. (2020). Sustainable supplier selection using combined FUCOM–Rough SAW model. *Reports in mechanical engineering*, *1*(1), 34-43. https://doi.org/10.31181/rme200101034c

[90] Ataei, Y., Mahmoudi, A., Feylizadeh, M. R., & Li, D. F. (2020). Ordinal priority approach (OPA) in multiple attribute decision-making. *Applied soft computing*, *86*, 105893. https://doi.org/10.1016/j.asoc.2019.105893

[91] Pamucar, D., Deveci, M., Gokasar, I., Işık, M., & Zizovic, M. (2021). Circular economy concepts in urban mobility alternatives using integrated DIBR method and fuzzy Dombi CoCoSo model. *Journal of cleaner production*, *323*, 129096. https://doi.org/10.1016/j.jclepro.2021.129096

[92] Mandal, K., & Basu, K. (2019). Vector aggregation operator and score function to solve multi-criteria decision making problem in neutrosophic environment. *International journal of machine learning and cybernetics*, *10*(6), 1373–1383. https://doi.org/10.1007/s13042-018-0819-4

[93] Spearman, C. (1961). The proof and measurement of association between two things. In *Studies in individual differences: The search for intelligence* (pp. 45–58). Appleton-Century-Crofts. https://doi.org/10.1037/11491-005.

[94] Sedgwick, P. (2012). Pearson's correlation coefficient. *Bmj*, *345*. https://doi.org/10.1136/bmj.e4483

[95] Fisher, R. A. (1925). *043: applications of" student's" distribution*. https://hekyll.services.adelaide.edu.au/dspace/bitstream/2440/15187/1/43.pdf

[96] Hu, J., Tan, Y., & Zou, W. (2021). Key factors influencing earthquake-induced liquefaction and their direct and mediation effects. *Plos one*, *16*(2), e0246387. https://doi.org/10.1371/journal.pone.0246387

[97] Uyanık, O. (2020). Soil liquefaction analysis based on soil and earthquake parameters. *Journal of applied geophysics*, *176*, 104004. https://doi.org/10.1016/j.jappgeo.2020.104004